Human neutrophils are not activated by Zika virus but reduce the infection of susceptible cells

Juliana Bernardi Aggio[1], Bárbara Nery Porto[2], Claudia Nunes Duarte dos Santos[1], Ana Luiza Pamplona Mosimann[1†*], Pryscilla Fanini Wowk[1†*]

[1] Laboratório de Virologia Molecular, Instituto Carlos Chagas, Fundação Oswaldo Cruz (FIOCRUZ), Curitiba, Brazil

[2] Department of Medical Microbiology and Infectious Diseases, University of Manitoba, Winnipeg, Canada

[†] These authors have contributed equally to this work and share senior authorship.

*** Correspondence:**

Pryscilla Fanini Wowk, Ana Luiza Pamplona Mosimann

pryscilla.wowk@fiocruz.br, ana.mosimann@fiocruz.br

Keywords: neutrophils, Zika virus, innate immunity, co-culture, NETs, migration.

Abstract

Zika virus (ZIKV) emergence highlighted the need for a deeper understanding on virus-host interaction to pave the development of antiviral therapies. The present work aimed to address the response of neutrophils during ZIKV infection. Neutrophils are an important effector cell in innate immunity involved in the host response to neurotropic arboviruses. Our results indicate that human neutrophils were not permissive to Asian or African ZIKV strains replication. Indeed, after stimulation with ZIKV, neutrophils were not primed against the virus as evaluated by the absence of CD11b modulation, secretion of inflammatory cytokines and granule content, production of reactive oxygen species and neutrophil extracellular traps formation. Overall, neutrophils did not affect ZIKV infectivity. Moreover, ZIKV infection of primary innate immune cells *in vitro* did not trigger neutrophil migration. However, neutrophil co-cultured with ZIKV susceptible cells (A549) resulted in lower frequencies of infection on A549 cells by cell-to-cell contact. *In vivo*, neutrophil depletion from immunocompetent mice did not affect ZIKV spreading to the draining lymph nodes. The data suggest human neutrophils do not play a *per se* antiviral role against ZIKV, but these cells might participate in an infected environment shaping the ZIKV infection in other target cells.

1 Introduction

Zika virus (ZIKV) is an enveloped vector-borne RNA virus, member of the genus *Flavivirus* which includes important human pathogens. The epidemic potential of flaviviruses is related to the global distribution of their arthropod vectors (mainly *Aedes* spp.), as well as human population density, mobility and anthropogenic interventions (1). Furthermore, mutation rate in the viral genome and the host immune-status may also impact on viral spread and pathogenesis (2). After decades of sparse reports of infection in Africa and Asia, since 2007 the ZIKV Asian genotype has been implicated in outbreaks in human populations, from Southeast Asia spreading throughout the Americas and reaching Europe (3). In Brazil, ZIKV was first detected in 2015 and recognized as a Public Health Emergency in 2016 (4). More than 220,000 cases were notified and the infection was associated with congenital diseases and to Guillain-Barré Syndrome in adults (5–7).

ZIKV infection has been reported to trigger a rapid recruitment and activation of monocytes, NK cells, plasmacytoid dendritic cells, and lymphocytes, and the upregulation of multiple signaling pathways, like pro-inflammatory cytokines and chemokines in the blood of non-human primates and humans (8–13). Among the innate immune cells, monocytes, dendritic cells and macrophages have been described as targets of ZIKV infection and replication (14–17). It has been suggested that the ensuing innate immune response can be associated with the fate of ZIKV disease. Cell infiltration and inflammation at ZIKV infection sites contributed to placental dysfunctions (18) and encephalitis (19–21). ZIKV affects adhesive properties of monocytes, enhancing their transmigration through endothelial barriers and viral dissemination to neural cells (22). Moreover, neutrophils, $Ly6C^{mid\text{-}hi}$ monocytes, and $CD45^{+}$ monocytes from AG129 mice (type I and II IFN receptor deficient), and bone marrow-derived S100A4+ macrophages from AG6 mice (type I, II and III IFN receptor deficient) were shown to be essential for ZIKV dissemination and pathogenesis in peripheral organs and testis (23–25). $CD45^{+}CD11b^{+}$ monocytes and macrophages play an important role in containing ZIKV spread in the placenta (26), while infected human placental macrophages might gain access to the fetus (27). In this context, the role played by neutrophils during ZIKV infection remains undetermined. Elucidating mechanisms by which neutrophils mediate an antiviral response may enable the development of therapies that retain antiviral functions but limit inflammation-associated damage.

Mature neutrophils are the most abundant granulocytes in the human bloodstream and the major effectors during inflammation and infection. Once in the infection site, neutrophils can rapidly

eliminate intra- and extracellular pathogens by phagocytosis, oxidative burst, multiple granule proteolytic enzymes, antimicrobial peptides and neutrophil extracellular traps (NETs) release (28,29). Neutrophils have been also recognized as multitasking cells capable of cross talking with adaptive responses, for example, presenting antigens during viral infections (30,31). The relevance of neutrophils during flaviviruses infection was demonstrated for *West Nile virus* (WNV) infections, where neutrophils act as Trojan horses carrying the virus into the central nervous system (CNS) enhancing WNV neuroinvasive disease (32). Neutrophil depletion prior to WNV infection resulted in reduced viremia and enhanced host survival (33).

Here, we address the role of neutrophils on ZIKV pathogenesis by the *in vitro* screening of classical human neutrophil defense mechanisms after stimulation with different ZIKV strains. We report that neutrophils are not targets for ZIKV replication nor good responder to ZIKV, yet neutrophils reduce ZIKV infection when in contact with target cells.

2 Materials and Methods

2.1 Cells

Human peripheral blood was obtained by intravenous puncture from healthy volunteers (both genders, aged between 21-50 years old and with no clinical evidence of disease) upon written consent. The procedures were in accordance with the Conselho Nacional de Ética em Pesquisa-CONEP (CAAE 60643816.6.0000.5248). Human neutrophils were isolated from peripheral blood by negative selection with magnetic microspheres MACSxpress Neutrophil Isolation Kit and MACSxpress Separator (Miltenyi Biotec), according to the manufacturer instructions. Cell viability was determined by Trypan blue exclusion assay and the neutrophil purification was confirmed by cytospin slides (Cytospin 4; Thermo Fisher Scientific) visualized by microscopy (LEICA AF6000 Modular System) (Figure 1A) and flow cytometry.

Peripheral blood mononuclear cells (PBMCs) were isolated using Histopaque density 1.077 g/mL (Lonza). $CD14^+$ cells were sorted with the MACS system (Miltenyi Biotec), according to the manufacturer instructions and seeded at $5x10^5$ cells/mL in RPMI-1640 media with L-glutamine (Lonza) supplemented with 10% fetal bovine serum (FBS; Gibco), 25 µg/mL gentamicin (Gibco), 100 IU/µg/mL penicillin-streptomycin (Sigma-Aldrich), 12.5 ng/mL recombinant human GM-CSF (PeproTech), and 25 ng/mL recombinant human IL-4 (PeproTech). The cells were incubated for 7 days at 37ºC, 5% CO_2 and humid atmosphere. On the third day of incubation, fresh supplemented

medium was added to the cell culture. Human monocyte-derived dendritic cells (mdDCs) differentiation was confirmed by flow cytometry ($CD11c^{+/high}CD14^{+/low}$).

Human A549 lung epithelial cells (ATCC CCL-185) were maintained in RPMI-1640 media supplemented with 10% FBS, 25 µg/mL gentamicin, and 100 IU/µg/mL penicillin-streptomycin at 37ºC, 5% CO_2 and humid atmosphere. *Aedes albopictus* mosquito C6/36 cells (ATCC CLR-1660) were grown in Leibovitz's media (L-15; Gibco) supplemented with 5% FBS, 25 µg/mL gentamicin, and 0.26% tryptose (Sigma-Aldrich) at 28°C.

2.2 Zika virus

Viral stocks of the ZIKV Asian strains, the clinical isolate BR 2015/15261 (34) and PE243 (35), and the ZIKV ancestral African isolate MR766 (36) were prepared in C6/36 cells. Seven days post-infection cell culture supernatant was collected, clarified by centrifugation and later titrated by foci-forming immunodetection assay in C6/36 cells (37). In parallel, C6/36 cells were maintained in the same conditions without viral addition. This conditioned supernatant, hereby called mock, was used as a negative control for cell activation and infection.

2.3 Cell interaction with ZIKV

Neutrophils at $2.5x10^5$ cells/200 µL of RPMI-1640 media supplemented with 25 µg/mL gentamicin and 100 IU/µg/mL penicillin-streptomycin were incubated for 2 hours with ZIKV strains (BR 2015/15261, PE243 and MR766) using a multiplicity of infection (MOI) of 1 at 37ºC, 5% CO_2 and humid atmosphere under agitation. As a control for cell activation, neutrophils were also incubated in the same conditions with mock, 100 ng/mL of *Escherichia coli* lipopolysaccharide (LPS-EK, InvivoGen), or 16 nM of phorbol 12-myristate 13-acetate (PMA; Sigma-Aldrich). After the 2h incubation period, neutrophils were washed twice (250 x *g*; 10 minutes) in non-supplemented media and seeded in 96-well plates in RPMI-1640 media supplemented with 10% FBS and antibiotics at 37ºC, 5% CO_2 and humid atmosphere. Supernatant collected right after the wash step was called input and used as a control to account for any remaining viruses in the neutrophil culture after washing out the initial inoculum (Figure 1B). Two (input), 6, 12 and 24 hours after the beginning of the stimulation, neutrophils and the culture supernatant were harvested and analysed. Supernatants were stored at -80ºC until further analysis. In some experiments, to exclude non-internalized virus binding in their surface, neutrophils were treated right after the wash steps (2 hours/input) with

0.05% trypsin-EDTA (Gibco) (Figure 1B) for 10 minutes at room temperature, followed by FBS addition, washed and suspended in the new media (38).

Chemokines in PBMCs and mdDCs culture supernatant were quantified 24 and 48 hours after ZIKV stimulation. For that, PBMCs (after isolation) and mdDCs (after 24 hours of resting) at $1x10^6$ cells/500 µL were stimulated with the same protocol described above for neutrophils (Figure 1B), but seeded in 24-well plates.

A549 and C6/36 cells were incubated for 2 hours with ZIKV strains (1 MOI) (or different stimuli when indicated) in 400 µL of media without FBS. After the incubation period, cells were washed twice with non-supplemented media and kept in media supplemented with 10% FBS and antibiotics during the indicated times.

2.4 Flow cytometry

Neutrophils and A549 cells viability were determined at the indicated time points using Annexin V (ImmunoTools) and 7-Amino-Actinomycin (7-AAD; BD Bioscience) following manufacturer's instructions (PE Annexin V Apoptosis Detection Kit; BD Bioscience). The frequency of ZIKV antigen in neutrophils, A549 cells and C6/36 cells was measured by staining with a flavivirus group specific envelope protein (E) monoclonal antibody 4G2 (ATCC HB-112) (37). Briefly, the cells were recovery, and if necessary were detached from the cell culture flask (A549 cells with trypsin and C6/36 with cell scraper), and blocked (5% FBS and 1% human AB serum in PBS) for 20 minutes at room temperature. Next, cells were fixed and permeabilized using the Cytofix/Cytoperm Fixation/Permeabilization Kit (BD Biosciences), stained with 4G2 FITC-conjugated antibody for 45 minutes at 37ºC, and washed twice. Alternatively, these cells were labeled with 4G2 antibody, goat anti-mouse Alexa Fluor 488 secondary antibody (Thermo Fisher Scientific) and Vybrant DyeCycleViolet Stain (Thermo Fisher Scientific), and fixed in slides pre-treated with poly-L-lysine (Sigma-Aldrich) for confocal microscopy imaging (LEICA SP5 AOBS). For surface markers staining, neutrophils were blocked and incubated with fluorochrome-conjugated mouse anti-human monoclonal antibodies specific for CD11b (clone ICRF44), CD16 (clone 3G8), CD62L (clone DREG-56) (BD Biosciences), and Hu Axl (clone D57HAXL) (eBioscience), for 20 minutes at room temperature. To measure intracellular reactive oxygen species generation, neutrophils were labeled with 0.5 µM of 5-(and-6)-chloromethyl-2',7'-dichlorodihydrofluorescein diacetate, acetyl ester (CM-H_2DCFDA) probe (Invitrogen) for 45 minutes at 37ºC. Cytokines and chemokines in the supernatant

of neutrophils, PBMCs and mdDCs culture supernatants were quantified by the Cytometric Bead Array (CBA) method using the Human Inflammatory Cytokines Kit and Human Chemokine Kit (BD Biosciences), following manufacturer's instructions. Flow cytometry was performed on a FACS Canto II with BD FACSDiva software (BD Biosciences) and the acquired data analyzed on FlowJoV10 (BD Biosciences).

2.5 RT-qPCR

Neutrophils RNA was extracted using the RNeasy Mini Kit (Qiagen) according to the manufacturer's instructions. RT-qPCR to detect ZIKV was performed in a 20 µL reaction final volume containing GoTaq one-step RT-qPCR master mix (Promega), 25 ng of sample RNA, 500 nM of the ZIKV1086 and ZIKV1162c oligonucleotides, and 200 nM of ZIKV1107-FAM probe according to a previously described protocol (39). RNase P (*RPPH1*) was used as a reference gene (40). All reactions were carried out in a LightCycler 96 System and the fluorescence threshold limit of the probe was automatically set by LightCycler software (Roche). The results were represented as the ΔCt between ZIKV and RNAase P amplification.

2.6 Neutrophil elastase measurement

Elastase was measured using the Human PMN-Elastase ELISA Kit (Invitrogen) in neutrophil culture supernatant at 6 hours after stimulation. Cell culture supernatant (100 µL) was added to a microwell plate coated with anti-human polymorphonuclear (PMN) elastase polyclonal antibody and incubated at room temperature for 1 hour with a Horseradish peroxidase-conjugated anti-α 1-proteinase inhibitor antibody. The immune complex was detected by adding tetramethyl-benzidine substrate solution and the absorbance was determined at 450 nm on a microplate reader (BioTek Synergy H1 Hybrid).

2.7 Neutrophil extracellular traps assessment

Neutrophils at $2x10^5$ cells/200 µL of RPMI-1640 media supplemented with antibiotics were incubated for 5 hours with either mock, ZIKV strains (1 MOI), or 160 nM of PMA in Lab-Tek chamber slides (Thermo Fisher Scientific) pre-treated with poly-L-Lysine at 37ºC, 5% CO_2 and humid atmosphere. For NETs visualization, the supernatant was carefully removed and the cells were fixed with 3% paraformaldehyde (Sigma-Aldrich), and stained with an anti-acetyl-histone H3 polyclonal antibody (Sigma) followed by a mouse anti-rabbit Alexa Fluor 488 secondary antibody

(Sigma) and Vybrant DyeCycleViolet Stain (Thermo Fisher Scientific) for 45 minutes at 37ºC. The slides were sealed with n-propyl gallate (Sigma-Aldrich) and observed by confocal microscopy (LEICA SP5 AOBS). For NETs quantification, following the stimulation period, neutrophils were treated with 0.04 U/µL of Turbo DNAse (Thermo Fisher Scientific) for 10 minutes at 37ºC. The enzymatic digestion was stopped with 5 mM EDTA (41). The culture was centrifuged (300 x g for 1 minute), the supernatant collected and 5-fold diluted. Free double-stranded DNA (dsDNA) was quantified using Quant-IT PicoGreen dsDNA kit (Invitrogen) in a Qubit 2.0 fluorometer (Invitrogen) according to the manufacturer's recommendations. To evaluate the effect of pre-formed PMA-induced NETs on viral particles capture, neutrophils were stimulated during 5 hours with media or PMA in the same conditions described above. Then, the culture was stimulated for 1 hour with ZIKV strains (1 MOI). Next, neutrophils were centrifuged (300 x g for 1 minute) and the supernatant (with virus not attached to the traps) collected and quantified by foci-forming immunodetection assay in C6/36 cells.

2.8 Neutrophil chemotaxis assay

Neutrophils at $3x10^5$ cells/200 µL of RPMI-1640 media supplemented with antibiotics were seeded on a 3 µm pore Thin Cert insert (Greiner Bio-One) coupled to a 24-well plate. Inducers of neutrophil chemotaxis were added to the bottom well in 600 µL of RPMI-1640 media containing 1,000 or 50,000 pg of recombinant human (rh-) IL-8 (PeproTech) or A549 cells culture previously infected for 48 hours with mock or ZIKV PE243 (1 MOI). For this specific experiment, infected A549 cells were maintained in the absence of FBS. RPMI-1640 media and A549 cells stimulated with mock were used as a negative control for cell migration. After 2 hours at 37ºC, 5% CO_2 and humid atmosphere, migratory neutrophils were collected from the bottom well system and the cell concentration determined by Turk dye counting. The chemotactic index was calculated as the ratio of the number of migratory neutrophils in each condition divided by the number of neutrophils that migrated in the negative control (42).

2.9 Co-culture assay

A549 cells (seeded in 24-well plates) at $1x10^5$ cells/ 400 µL in RPMI-1640 media supplemented with antibiotics were stimulated for 2 hours with mock or ZIKV strains (1 MOI) in the absence or presence of neutrophils of a ratio of 1:5. Afterwards, neutrophils were assessed for surface markers by flow cytometry as described above, and A549 cells were washed twice and kept in 500 µL of

RPMI-1640 media supplemented with 10% FBS and antibiotics for 16 hours. At the end of the 18 hours of infection, A549 cells were assessed for viability and intracellular ZIKV antigen by flow cytometry. To evaluate if neutrophils were physically interacting with A549 cells through surface proteins, in some experiments, before adding A549 cells cells culture, neutrophils were treated with trypsin for 10 minutes at room temperature, added FBS, washed and suspended in fresh media. In a different co-culture experiment setting, A549 cells were incubated for 2 hours with mock or ZIKV strains (1 MOI), washed twice and incubated for 24 hours. Then, neutrophils in a ratio of 1:5 were added or not to these cultures for 16 hours. At the end of the 40 hours of infection, A549 cells were evaluated for frequency of ZIKV antigen.

2.10 *In vivo* ZIKV infection model

C57BL/6 mice were obtained from Instituto Carlos Chagas/FIOCRUZ-PR animal facility, and maintained and handled according to the directives of the Guide for the Care and Use of Laboratory Animals of the Brazilian National Council of Animal Experimentation. The protocols were approved by the Committee on the Ethics of Animal Experimentation from Fundação Oswaldo Cruz – CEUA/FIOCRUZ (license LW 03-19). Both male and female mice between 8-12-week-old were infected subcutaneously in the hind footpad with ZIKV PE243 ($5x10^5$ FFU, 10 µL) to determine systemic ZIKV titers. After 10 minutes, 1, 3, 6 and 24 hours of infection, spleen, kidney and lymph nodes (popliteal (pLN), lumbar aortic (laLN), and sciatic lymph nodes (sLN)) were aseptically removed, homogenized using a tissue grinder, submitted to three freeze-thaw cycles and the viral load measured by foci-forming immunodetection assay in C6/36 cells. Both ipsi- and contralateral lymph nodes per animal were pooled together. Blood was collected through cardiac puncture at the same time points and plasma viremia was titrated in C6/36 cells.

To evaluate the neutrophil influence in ZIKV spread to peripheral organs, neutrophils were depleted and the animals infected with ZIKV. Animals were inoculated intraperitoneally with 200 µL of PBS containing 400 µg of anti-mouse Ly6G (clone 1A8; BioxCell) or mouse IgG2a isotype control (clone C1.18.4; BioxCell). Control animals received 200 µL of PBS (Lonza). After 18 hours, the frequency of neutrophils in total blood was evaluated through flow cytometry by surface staining with fluorochrome-conjugated anti-mouse monoclonal antibodies specific for CD11b (clone M1/70), and Ly6C/G (clone RB6-8C5) (BD Biosciences). Neutrophil-depleted animals were inoculated in the hind footpad with PBS only or 1,000 ng of LPS (to induce an inflammatory environment). After 3 hours, mice were inoculated with 10 µL of ZIKV PE243 ($1.3x10^6$ FFU) in the same footpad. One

hour later, popliteal lymph nodes (pLNs) were pooled, harvested and the viral title determined as above.

2.11 Statistical Analyses

Analyses were performed using GraphPad Prism 8 (GraphPad Software, Inc.). Wilcoxon matched-pairs signed rank test (nonparametric paired t-test) was used in the analysis of the *in vitro* experiments with primary human cells to clarify individual patterns. One-way Anova with Tukey's multiple comparison test was used in animal experiments to compare the average of groups. A cut-off of $p < 0.05$ was considered significant.

3 Results

3.1 ZIKV does not establish a productive infection in human neutrophils

We first evaluate whether any of the tested ZIKV strains trigger human neutrophil death until 24 hours after stimulation (Figure 1B). It was observed a similar exposition of phosphatidylserine between mock- and the ZIKV strains-stimulated neutrophils over time and low loss of cellular integrity indicated by 7-AAD uptake (Supplementary Figure 1). The observed neutrophil phenotype concurs with previous knowledge that in the absence of inflammation, neutrophils have a short life span and undergo constitutive apoptosis (43), and LPS, that is a positive control of neutrophil activation, restricted apoptosis at the late time points (44).

Viruses, in addition to subverting the target cell into a reservoir for replication and dissemination, may use the infected cells as a Trojan horse to overcome physiological host defense barriers (32). The infection can also result in the inhibition of important cell signal transduction pathways (17). To address this issue, we sought to understand whether human neutrophils are susceptible to and sustain ZIKV infection. No positive cells for the intracellular staining of the ZIKV E protein (4G2 antibody) were detected 24 hours after stimulation with the three ZIKV strains tested through immunofluorescence or flow cytometry (Figure 1C and 1D). It contrasts with the infection observed in the highly permissive mosquito cell line C6/36 (Figure 1C and 1D). The possibility of an active internalization of a few viral particles by neutrophils via receptors or phagocytosis could not be excluded, even though we reported the absence of AXL in the surface of human neutrophils, which was expressed in the ZIKV susceptible human lineage A549 (Figure 1E). Indeed, ZIKV RNA could be detected in neutrophils incubated with the viruses (Figure 1F). However, we did not observe a

significant increase in ZIKV RNA levels over time (Figure 1F) nor the release of functional viral particles in loads greater than the input (Figure 1G). Treatment of neutrophils with trypsin after the wash steps resulted in the reduction but not in the abolishment of virus RNA levels (Figure 1H). This suggests that the low RNA levels measured cannot be fully attributed to viral inoculum leftover, and at least partially, could be explained by the virus particles that stick at the cell membrane.

3.2 Human neutrophils are mild responsive to direct contact with ZIKV

The recognition of viral elements in the cell cytosol triggers defense mechanisms involved in viral replication control and inflammation. However, a significant part of neutrophil activation mechanisms is coordinated through the signaling of cell surface receptors (43). Following the experimental setting in Figure 1B, the expression of the adhesion integrin CD11b was upregulated over time following LPS stimulation, while the selectin adhesion receptor CD62L was downregulated (Figure 2A-C), indicating priming of neutrophils (45,46). Nevertheless, no differences were observed in the expression of CD11b molecule between mock- and the ZIKV strains-stimulated neutrophils (Figure 2B), and only slight differences were observed in the expression of CD62L (Figure 2C). No significant differences were observed in the IL-8/CXCL8 levels secreted by neutrophils after 24 hours of stimulation between mock and ZIKV (Figure 2D). Similar results were obtained for IL-1β, IL-6 and IL-10 (data not shown). The low levels of elastase detected in neutrophils culture supernatant after 6 hours of stimulation with ZIKV BR 2015/15261 were similar to mock-stimulated cells (Figure 2E). It was also noted an overall low production of ROS in neutrophils after ZIKV stimulation, measured by the oxidation of chloromethyl-H_2DCFDA (Figure 2A and 2F), in contrast to the oxidative stress generated by PMA stimulation, a well-known ROS inducer. We confirmed that NETs were not induced by any ZIKV strains tested after 5 hours of stimulation through the absence of web-link extracellular structures colocalizing with DNA and histone (Figure 3A) and the absence of free DNA in neutrophil supernatants (Figure 3B). PMA is a robust NET inducer over a 3-4 hour time course via ROS (47), as observed here (Figure 3A-B). Moreover, ZIKV was not trapped by NETs, as the same loads of ZIKV were quantified in the supernatant of neutrophils stimulated or not with PMA (Figure 3C). To confirm that neutrophil does not impact ZIKV particles, neutrophils were stimulated for 6 hours with ZIKV, and the free virus recovered from the supernatant did not have impaired infectivity in a subsequent infection of susceptible cells (Figure 4).

3.3 ZIKV infection does not provide a favorable environment for human neutrophil migration

Although neutrophils are circulatory cells and therefore have the potential to encounter viruses in the bloodstream, their fate is to contribute to the inflammation on the infected tissue. In fact, the priming of neutrophils in the circulation by an isolated stimulus is insufficient, and their complete activation to full capacity is a multistep process achieved after their transmigration through the endothelium following a chemotactic gradient (43). Secretion of IL-8/CXCL8, an important human neutrophil chemoattractant, was measured after ZIKV stimulation of mdDCs and PBMCs for 24 and 48 hours. LPS was used as a positive control of activation and boosted the chemokines production (Figure 5A). A concentration of recombinant human IL-8 (rhIL-8) corresponding approximately to the ones detected in the mdDCs and PBMCs supernatant (1,000 pg) was not enough to induce neutrophil migration in a transwell assay (Figure 5B). Neutrophils migrated with a 50-fold higher rhIL-8 concentration (Figure 5B). Interestingly, a more permissive cell line, A549 cells, when infected with ZIKV PE243 for 48 hours, also did not promote neutrophil migration (Figure 5B).

3.4 Human neutrophils reduce ZIKV infection in A549 by cell-cell contact

To mimic a situation where neutrophils reached an infected environment after migration, we co-cultured neutrophils with A549 cells. Neutrophils were added to A549 cells concomitant with ZIKV infection. Both stimuli were maintained for 2 hours and then removed. The A549 cells infection frequency was evaluated 16 hours after the removal of the viral input by the detection of ZIKV E protein (4G2) (Figure 6A). A significant reduction in A549 cell infection was observed when neutrophils were added during the infection time (Figure 6A and 6B). We did not detect a reduction in the frequency of A549 cells annexin V^{-}7-AAD^{-} due to neutrophil presence (Figure 6C). We previously hypothesized that a small number of particles might have been internalized by neutrophils and a reduced fraction of the virus particles could be binding to the neutrophils surface. Nevertheless, such a small reduction in the number of free viral particles is not enough to explain the decrease in the infection rate observed in the co-culture. Besides, no decrease in A549 infection was detected when ZIKV was pre-incubated with neutrophils (Figure 4). Neutrophils co-cultured with A549 cells did not modulate CD11b and CD62L receptors (Figure 6D and 6E), indicating the reduction of the infection is not due to neutrophils activation. However, neutrophil treatment with trypsin before addition to A549 cells restored A549 cells infection frequencies and replication (Figure 6A, 6F and 6G). Therefore, we hypothesized that neutrophils were interacting with A459 cells through surface

protein membrane components and impairing ZIKV infection. The treatment with trypsin did not significantly affect the viability of neutrophils (annexin V^-7-AAD^-) (Figure 7A), nor the expression of CD11b (Figure 7B and C), but significantly reduce the expression of CD62L on neutrophils (Figure 7B and 7D), suggesting an impact on neutrophil surface proteins by trypsin. In an alternative co-culture setting, aimed to mimic the neutrophil role to an established ZIKV infection, A549 cells were infected for 24 hours with ZIKV strains and after this time neutrophils were added to the culture for 16 hours. Even in a scenario where infection was already established, a significant reduction in the frequency of ZIKV infection was observed after neutrophils addition (Supplementary Figure 2).

3.5 Neutrophil depletion does not alter ZIKV titers in the draining lymph node

After subcutaneous infection in the hind footpad, ZIKV PE243 were detected only up to 3 hours after infection in the lymph nodes (popliteal (pLN), lumbar aortic (laLN), and sciatic lymph nodes (sLN)) of C57BL/6 immunocompetent mice (Figure 8A). ZIKV PE243 were not detected in the spleen, kidney or blood of these animals in any of the assessed times. Therefore, we used the pLN 1 hour of ZIKV infection as a viral spread indicator site in our subsequent studies. C57BL/6 mice had neutrophils significantly reduced through pre-treatment with a monoclonal antibody targeting Ly6G (Figure 8B and 8C). Eighteen hours post-neutrophil depletion treatment and 3 hours prior to ZIKV PE243 subcutaneous infection, mice were inoculated subcutaneously in the hind footpad with LPS to stimulate cell migration to the injection site (Figure 8D). The animals treated with the anti-Ly6G antibody (Ly6G x LPS) presented similar titers of ZIKV in the pLN than animals that received no antibody treatment (PBS x LPS) (Figure 8D). The slightly reduced titers in the pLN seen in mice that received LPS in comparison with the ones that received PBS in the footpad were attributed to the inflammatory context. This result suggests that, in this model, the presence of neutrophils was not essential to contain ZIKV spread to the draining lymph node.

4 Discussion

Neutrophil-inflammatory responses triggered by viral infection are necessary for an effective antiviral immunity (48–51), but can also become dysregulated and result in tissue injury (52,53). This concept could be extended to ZIKV pathology, in which neutrophils could be associated with the virus neurotropic nature, the ability to cause injury to the reproductive tract and be sexually transmitted, as well as the long-term viral persistence in some body fluids and tissues (3). In order to

investigate these possibilities, we interrogated the response of human neutrophils to Asian and African ZIKV strains in a diverse experimental setting.

Neutrophils were suggested to be permissive to ZIKV as viral RNA was found in myeloperoxidase$^+$ neutrophils present in the lymph nodes of cynomolgus macaques 7 days post-infection (10), and in CD45$^+$CD11b$^+$ neutrophil-myeloid cells in the placenta of AIR mice (vertical transmission model in a *Rag1*-deficient mouse) (26). In contrast to those previous findings, our results shown that, beside some ZIKV RNA detection, human neutrophils do not appear to support any significant ZIKV replication and do not represent a remarkable ZIKV reservoir. This is in agreement with previous reports demonstrating that ZIKV preferentially targets CD14$^+$CD16$^+$ monocytes in the blood (16). Also according to our data, AXL, a TAM family tyrosine kinase that has been described as a facilitator of ZIKV infection due to attenuation of type I IFN (54), was found to be absent from neutrophils surface. Nevertheless, ZIKV receptors and co-receptors are still not well characterized and AXL is one of the cell surface molecules that could help mediate ZIKV infection.

Surprisingly, stimulation of neutrophil with ZIKV did not promote a strong cell activation or any of the classical neutrophil microbicidal mechanisms as noted by the absence of CD11b modulation, secretion of inflammatory cytokines and elastase, production of reactive oxygen species and NETs. These results indicate neutrophils that presented a non-responsive phenotype in our experimental settings and would not be the major source of inflammatory mediators during ZIKV infection. Other viruses, such as *Human immunodeficiency virus-1*, induced activation on neutrophils by modulating the expression of several Toll-like receptors, CD11b and CD62, promoting the secretion of IL-6 and TNF-α, and altering ROS production (55). According to our results, ZIKV and *Dengue virus* type 2 were previously shown not be able to provoke NETs induction in mice (56). Interestingly, our data pointed out that ZIKV particles are not captured by NETs in a context of the DNA web induced by a secondary stimulus. Zanluqui *et al*. preprint manuscript (57), also addresses the role played by neutrophils during ZIKV infection. Corroborating our finds, the authors shown the lack of ZIKV interference in human neutrophil viability and NETs release, as well as mice neutrophils did not display a pro-inflammatory profile and ROS production against the virus (57). A viral escape from innate immune components could result in delayed immune responses favoring virus spread. Furthermore, we cannot rule out a possible suppression of neutrophil action by ZIKV, as already shown for primary monocytes, mdDCs and plasmacytoid DCs that have their maturation and

activation impaired during ZIKV replication (14,16,17,58,59). Moreover, a cohort of rhesus monkeys produced minimal systemic cytokine response to ZIKV infection (9).

Furthermore, several reports have indicated that neutrophils migrate to different tissues during ZIKV infection in IFN receptor-deficient mouse, such CNS, spleen, spinal cord, epididymis, and testis (19,20,24,60,61), and in humans and non-human primates mucosa, placenta, and fetus (11,62,63). Patients during acute or recovery disease phase, THP-1 cells and monocytes secrete increased amounts IL-8/CXCL8 following ZIKV infection (12,13,16,64). Moreover, myeloid cells in AG129 mice challenged with ZIKV were responsible for the production of cytokines involved in leukocyte recruitment and viral dissemination to peripheral organs (23). Despite these reports, in our settings, 48 hours of ZIKV infection of mdDCs and PBMCs did not induce sufficient levels of IL-8 to promote neutrophil migration *in vitro*. Even in ZIKV infected A549 cells, that endure high levels of viral replication and can generate a more complex environment, the neutrophil migration is not promoted. Frumence *et al*. (65) shown the secretion of soluble IL-8 in ZIKV infected A549 cells, however at low levels, confirming that the *in vitro* assay we used presents limitations in order to promote neutrophil migration.

In an attempt to assess the putative impact of neutrophil migration to infected tissues *in vitro*, we used a co-culture system with A549 cells. Our results show a reduction in the rate of ZIKV infection of A549 cells when neutrophils are present at the moment of the infection or in a pre-established infection. This infection impairment seems not to be related to neutrophil activation, but due to a physical interaction between surface molecules in both cells. It has been shown that cell-to-cell contact between neutrophils and A549 cells leads to a pro-proliferative effect on these cells involving the release of elastase and COX-2 products by neutrophils (66). An increase in the production of IL-6 and IL-8 by A549 cells (67), and induction of A549 cell death by apoptotic neutrophils by soluble Fas ligand (68) have also been reported. However, it was not the case in our model, where neutrophil presence did not affect A549 cell viability. The loss of CD62L in neutrophils after treatment with trypsin, a condition in which the frequency of ZIKV infection were restored in A549 cells, might bear a connection to the pathways involved in the neutrophil modulation of ZIKV infection in A549 cells. Herbert *et al*. (69) have reported that the β2- integrin ligand LFA-1 on neutrophils binds to the ICAM-1 receptor on epithelial cells and mediate, at least in part, epithelial damage, neutrophil degranulation and reduction of *Respiratory syncytial virus* (RSV) load. It remains to be defined what molecules and pathways might be involved during these cell-cell interactions that potentially

417 contribute to the reduction of viral infection and proliferation and that could be explored in the future
418 as targets against flavivirus infection. Secondary action of neutrophils in the site of infection is linked
419 to the mosquito saliva components. During *Semliki Forest virus* infection, the mosquito bite induced
420 a neutrophil influx at the site of the bite, and these cells helped coordinate the entry of susceptible
421 myeloid cells that are permissive to viral infection (70).

422 Finally, in order to gain a better understanding on the role played by neutrophils in ZIKV clearance at
423 the inflammation site, we depleted neutrophils from C57BL/6 mice. In this scenario, we did not
424 observe a direct action of neutrophils in preventing ZIKV spread to the lymph nodes in the first hour
425 after ZIKV inoculation in a setting where an inflammatory environment had been previously induced
426 by LPS injection. Interestingly, other authors reported that besides an extensive neutrophil
427 recruitment to the inflammation site after certain virus infections (RSV, *Herpes simplex virus type 1*
428 and *Coxsackievirus B3*), neutrophils did not play an important role in viral replication and disease
429 susceptibility, which in turn was exerted by monocytes and macrophages (71–74).

430 Immunocompetent mice, like C57BL/6 strain, readily resolve ZIKV infection and might be a limited
431 model to answer long-term questions. However, IFN pathway deficient models, despite being
432 valuable tools to study ZIKV pathology, could bear differences in the kinetics of neutrophil
433 recruitment. Intracranial ZIKV infection in C57BL/6 WT or $Rag1^{-/-}$ mice (deficient in mature T and
434 B cells) resulted in a lethal encephalitis with infiltration of macrophages and NK cells (19). Neonatal
435 immunocompetent mice challenged subcutaneously with ZIKV elicit $CD8^{+}$ T cells to the CNS (20).
436 In contrast, $IFNAR^{-/-}$ mice (IFN type I and II receptor deficient) infected by both routes, shown an
437 accelerated ZIKV spread to peripheral organs and to the CNS, where it elicits an inflammatory
438 response characterized by neutrophils infiltration (19,20). In the context of infection with the
439 pulmonary bacteria *Francisella tularensis* and *Influenza virus*, the absence of IFN-I results in higher
440 neutrophil recruitment (75,76). It would be of considerable interest to assess the production of
441 neutrophil chemoattractants following ZIKV infection in the CNS of humans *pos mortem*, since
442 ZIKV antagonizes human IFN-I (77).

443 In conclusion, the results indicate that human neutrophils are slightly activated by direct contact with
444 ZIKV. However, the direct interaction between ZIKV and neutrophils does not contribute to the viral
445 replication or to the inflammatory disease associated with the virus infection. Conversely, human
446 neutrophils are able to reduce ZIKV infection and replication on A549 cells. It is not yet clear
447 though, what is the mechanistically role of neutrophils in this context. Finally, despite not being a

target cell for ZIKV infection, our data suggest that, *in vitro*, neutrophils play a role in shaping ZIKV infection in other target cells.

Conflict of Interest

The authors have no financial conflicts of interest.

Author Contributions

JBA and PFW conceptualized, designed, and performed the experiments and data analysis. BNP and ALMP contributed to the interpretation and discussion of the data. CNDS contributed with her expertise in virology. All authors prepared the manuscript.

Funding

This research was funded by the Conselho Nacional de Desenvolvimento Científico e Tecnológico (CNPq-Universal - 444857/2014-1) and by Instituto Carlos Chagas/Fiocruz-PR (CNPq – PROEP-ICC 442356/2019-6). CNDS (307176/2018-5) is a CNPq fellow.

Acknowledgments

We thank Instituto Carlos Chagas's staff and colleagues at the Molecular Virology Laboratory for technical assistance, and Juliano Bordignon for critical reading. We also thank the Program for Technological Development in Tools for Health – PDTIS/FIOCRUZ for the use of the Flow Cytometry (RPT08L), Microscopy (RPT07C), and Animal facilities at Instituto Carlos Chagas/Fiocruz-PR.

References

1. Olson MF, Juarez JG, Kraemer MUG, Messina JP, Hamer GL. Global patterns of aegyptism without arbovirus. *PLoS Negl Trop Dis* (2020) **15**:e0009397. doi:10.1101/2020.07.20.212209

2. Pierson TC, Diamond MS. The continued threat of emerging flaviviruses. *Nat Microbiol* (2020) **5**:796–812. doi:10.1038/s41564-020-0714-0

3. Pierson TC, Diamond MS. The emergence of Zika virus and its new clinical syndromes. *Nature* (2018) **560**:573–581. doi:10.1038/s41586-018-0446-y

4. Zanluca C, de Melo VCA, Mosimann ALP, dos Santos GIV, dos Santos CND, Luz K. First report of autochthonous transmission of Zika virus in Brazil. *Mem Inst Oswaldo Cruz* (2015) **110**:569–572. doi:10.1590/0074-02760150192

5. Cugola FR, Fernandes IR, Russo FB, Freitas BC, Dias JLM, Guimarães KP, Benazzato C, Almeida N, Pignatari GC, Romero S, et al. The Brazilian Zika virus strain causes birth defects in experimental models. *Nature* (2016) **534**:267–271. doi:10.1038/nature18296

6. Cao-Lormeau V-M, Blake A, Mons S, Lastère S, Roche C, Vanhomwegen J, Dub T, Baudouin L, Teissier A, Larre P, et al. Guillain-Barré Syndrome outbreak associated with Zika virus infection in French Polynesia: a case-control study. *Lancet* (2016) **387**:1531–1539. doi:10.1016/S0140-6736(16)00562-6

7. Faria NR, Azevedo R do S da S, Kraemer MUG, Souza R, Cunha MS, Hill SC, Thézé J, Bonsall MB, Bowden TA, Rissanen I, et al. Zika virus in the Americas: Early epidemiological and genetic findings. *Science (80-)* (2016) **352**:345–349. doi:10.1126/science.aaf5036

8. Aid M, Abbink P, Larocca RA, Boyd M, Nityanandam R, Nanayakkara O, Martinot AJ, Moseley ET, Blass E, Borducchi EN, et al. Zika Virus Persistence in the Central Nervous System and Lymph Nodes of Rhesus Monkeys. *Cell* (2017) **169**:610–620. doi:10.1016/j.cell.2017.04.008

9. Hirsch AJ, Smith JL, Haese NN, Broeckel RM, Parkins CJ, Kreklywich C, DeFilippis VR, Denton M, Smith PP, Messer WB, et al. Zika Virus infection of rhesus macaques leads to viral persistence in multiple tissues. *PLoS Pathog* (2017) **13**:e1006219. doi:10.1371/journal.ppat.1006219

10. Osuna CE, Lim SY, Deleage C, Griffin BD, Stein D, Schroeder LT, Omange R, Best K, Luo M, Hraber PT, et al. Zika viral dynamics and shedding in rhesus and cynomolgus macaques. *Nat Med* (2016) **22**:1448–1455. doi:10.1038/nm.4206

11. O'Connor MA, Tisoncik-Go J, Lewis TB, Miller CJ, Bratt D, Moats CR, Edlefsen PT, Smedley J, Klatt NR, Gale M, et al. Early cellular innate immune responses drive Zika viral persistence and tissue tropism in pigtail macaques. *Nat Commun* (2018) **9**:3371. doi:10.1038/s41467-018-05826-w

12. Kam Y-W, Leite JA, Lum FM, Tan JJL, Lee B, Judice CC, De Toledo Teixeira DA, Andreata-Santos R, Vinolo MA, Angerami R, et al. Specific Biomarkers Associated With Neurological Complications and Congenital Central Nervous System Abnormalities From Zika Virus-Infected Patients in Brazil. *J Infect Dis* (2017) **216**:172–181. doi:10.1093/infdis/jix261

13. Lum FM, Lye DCB, Tan JJL, Lee B, Chia PY, Chua TK, Amrun SN, Kam YW, Yee WX, Ling WP, et al. Longitudinal Study of Cellular and Systemic Cytokine Signatures to Define the Dynamics of a Balanced Immune Environment During Disease Manifestation in Zika Virus–Infected Patients. *J Infect Dis* (2018) **218**:814–824. doi:10.1093/infdis/jiy225

14. Bowen JR, Quicke KM, Maddur MS, O'Neal JT, McDonald CE, Fedorova NB, Puri V, Shabman RS, Pulendran B, Suthar MS. Zika Virus Antagonizes Type I Interferon Responses during Infection of Human Dendritic Cells. *PLoS Pathog* (2017) **13**:e1006164. doi:10.1371/journal.ppat.1006164

15. Foo S-S, Chen W, Chan Y, Bowman JW, Chang L-C, Choi Y, Yoo JS, Ge J, Cheng G, Bonnin A, et al. Asian Zika virus strains target CD14+ blood monocytes and induce M2-skewed immunosuppression during pregnancy. *Nat Microbiol* (2017) **2**:1558–1570.

doi:10.1038/s41564-017-0016-3

16. Michlmayr D, Andrade P, Gonzalez K, Balmaseda A, Harris E. CD14+CD16+ monocytes are the main target of Zika virus infection in peripheral blood mononuclear cells in a paediatric study in Nicaragua. *Nat Microbiol* (2017) **2**:1462–1470. doi:10.1038/s41564-017-0035-0

17. Vielle NJ, Zumkehr B, García-Nicolás O, Blank F, Stojanov M, Musso D, Baud D, Summerfield A, Alves MP. Silent infection of human dendritic cells by African and Asian strains of Zika virus. *Sci Rep* (2018) **8**:5440. doi:10.1038/s41598-018-23734-3

18. Hirsch AJ, Roberts VHJ, Grigsby PL, Haese N, Schabel MC, Wang X, Lo JO, Liu Z, Kroenke CD, Smith JL, et al. Zika virus infection in pregnant rhesus macaques causes placental dysfunction and immunopathology. *Nat Commun* (2018) **9**:263. doi:10.1038/s41467-017-02499-9

19. Hayashida E, Ling ZL, Ashhurst TM, Viengkhou B, Jung SR, Songkhunawej P, West PK, King NJC, Hofer MJ. Zika virus encephalitis in immunocompetent mice is dominated by innate immune cells and does not require T or B cells. *J Neuroinflammation* (2019) **16**:177. doi:10.1186/s12974-019-1566-5

20. Manangeeswaran M, Ireland DDC, Verthelyi D. Zika (PRVABC59) Infection Is Associated with T cell Infiltration and Neurodegeneration in CNS of Immunocompetent Neonatal C57Bl/6 Mice. *PLoS Pathog* (2016) **12**:e1006004. doi:10.1371/journal.ppat.1006004

21. Tripathi S, Balasubramaniam VRMT, Brown JA, Mena I, Grant A, Bardina S V., Maringer K, Schwarz MC, Maestre AM, Sourisseau M, et al. A novel Zika virus mouse model reveals strain specific differences in virus pathogenesis and host inflammatory immune responses. *PLoS Pathog* (2017) **13**:e1006258. doi:10.1371/journal.ppat.1006258

22. Ayala-Nunez NV, Follain G, Delalande F, Hirschler A, Partiot E, Hale GL, Bollweg BC, Roels J, Chazal M, Bakoa F, et al. Zika virus enhances monocyte adhesion and transmigration favoring viral dissemination to neural cells. *Nat Commun* (2019) **10**:4430. doi:10.1038/s41467-019-12408-x

23. McDonald EM, Anderson J, Wilusz J, Ebel GD, Brault AC. Zika virus replication in myeloid cells during acute infection is vital to viral dissemination and pathogenesis in a mouse model. *J Virol* (2020) **94**:e00838-20. doi:10.1128/JVI.00127-20

24. McDonald EM, Duggal NK, Ritter JM, Brault AC. Infection of epididymal epithelial cells and leukocytes drives seminal shedding of Zika virus in a mouse model. *PLoS Negl Trop Dis* (2018) **12**:e0006691. doi:10.1371/journal.pntd.0006691

25. Yang W, Wu YH, Liu SQ, Sheng ZY, Zhen Z Da, Gao RQ, Cui XY, Fan DY, Qin ZH, Zheng AH, et al. S100A4+ macrophages facilitate zika virus invasion and persistence in the seminiferous tubules via interferon-gamma mediation. *PLoS Pathog* (2020) **16**:e1009019. doi:10.1371/journal.ppat.1009019

26. Winkler CW, Evans AB, Carmody AB, Peterson KE. Placental Myeloid Cells Protect against Zika Virus Vertical Transmission in a Rag1-Deficient Mouse Model. *J Immunol* (2020) **205**:143–152. doi:10.4049/jimmunol.1901289

555 27. de Noronha L, Zanluca C, Azevedo MLV, Luz KG, dos Santos CND. Zika virus damages the
556 human placental barrier and presents marked fetal neurotropism. *Mem Inst Oswaldo Cruz*
557 (2016) **111**:287–293. doi:10.1590/0074-02760160085

558 28. Brinkmann V, Reichard U, Goosmann C, Fauler B, Uhlemann Y, Weiss DS, Weinrauch Y,
559 Zychlinsky A. Neutrophil Extracellular Traps Kill Bacteria. *Science (80-)* (2004) **303**:1532–
560 1535. doi:10.1126/science.1092385

561 29. Kruger P, Saffarzadeh M, Weber ANR, Rieber N, Radsak M, von Bernuth H, Benarafa C,
562 Roos D, Skokowa J, Hartl D. Neutrophils: Between Host Defence, Immune Modulation, and
563 Tissue Injury. *PLoS Pathog* (2015) **11**:e1004651. doi:10.1371/journal.ppat.1004651

564 30. Duffy D, Perrin H, Abadie V, Benhabiles N, Boissonnas A, Liard C, Descours B, Reboulleau
565 D, Bonduelle O, Verrier B, et al. Neutrophils Transport Antigen from the Dermis to the Bone
566 Marrow, Initiating a Source of Memory CD8+ T Cells. *Immunity* (2012) **37**:917–929.
567 doi:10.1016/j.immuni.2012.07.015

568 31. Hufford MM, Richardson G, Zhou H, Manicassamy B, García-Sastre A, Enelow RI, Braciale
569 TJ. Influenza-Infected Neutrophils within the Infected Lungs Act as Antigen Presenting Cells
570 for Anti-Viral CD8+ T Cells. *PLoS One* (2012) **7**:e46581. doi:10.1371/journal.pone.0046581

571 32. Paul AM, Acharya D, Duty L, Thompson EA, Le L, Stokic DS, Leis AA, Bai F. Osteopontin
572 facilitates West Nile virus neuroinvasion via neutrophil "Trojan horse" transport. *Sci Rep*
573 (2017) **7**:4722. doi:10.1038/s41598-017-04839-7

574 33. Bai F, Kong K, Dai J, Qian F, Zhang L, Brown CR, Fikrig E, Montgomery RR. A Paradoxical
575 Role for Neutrophils in the Pathogenesis of West Nile Virus. *J Infect Dis* (2010) **202**:1804–
576 1812. doi:10.1086/657416

577 34. Strottmann DM, Zanluca C, Mosimann ALP, Koishi AC, Auwerter NC, Faoro H, Cataneo
578 AHD, Kuczera D, Wowk PF, Bordignon J, et al. Genetic and biological characterization of
579 Zika virus isolates from different Brazilian regions. *Mem Inst Oswaldo Cruz* (2019)
580 **114**:e190150. doi:10.1590/0074-02760190150

581 35. Donald CL, Brennan B, Cumberworth SL, Rezelj V V., Clark JJ, Cordeiro MT, Freitas de
582 Oliveira França R, Pena LJ, Wilkie GS, Da Silva Filipe A, et al. Full Genome Sequence and
583 sfRNA Interferon Antagonist Activity of Zika Virus from Recife, Brazil. *PLoS Negl Trop Dis*
584 (2016) **10**:e0005048. doi:10.1371/journal.pntd.0005048

585 36. Dick GWA, Kitchen SF, Haddow AJ. Zika virus isolation and serological specificity. *Trans R*
586 *Soc Trop Med Hyg* (1952) **46**:509–520.

587 37. Cataneo AHD, Kuczera D, Koishi AC, Zanluca C, Silveira GF, Arruda TB de, Suzukawa AA,
588 Bortot LO, Dias-Baruffi M, Verri WA, et al. The citrus flavonoid naringenin impairs the in
589 vitro infection of human cells by Zika virus. *Sci Rep* (2019) **9**:16348. doi:10.1038/s41598-019-
590 52626-3

591 38. Dejarnac O, Hafirassou ML, Chazal M, Versapuech M, Gaillard J, Perera-Lecoin M, Umana-
592 Diaz C, Bonnet-Madin L, Carnec X, Tinevez JY, et al. TIM-1 Ubiquitination Mediates
593 Dengue Virus Entry. *Cell Rep* (2018) **23**:1779–1793. doi:10.1016/j.celrep.2018.04.013

39. Lanciotti RS, Kosoy OL, Laven JJ, Velez JO, Lambert AJ, Johnson AJ, Stanfield SM, Duffy MR. Genetic and Serologic Properties of Zika Virus Associated with an Epidemic, Yap State, Micronesia, 2007. *Emerg Infect Dis* (2008) **14**:1232–1239. doi:10.3201/eid1408.080287

40. Emery SL, Erdman DD, Bowen MD, Newton BR, Winchell JM, Meyer RF, Tong S, Cook BT, Holloway BP, McCaustland KA, et al. Real-Time Reverse Transcription-Polymerase Chain Reaction Assay for SARS-associated Coronavirus. *Emerg Infect Dis* (2004) **10**:311–316. doi:10.3201/eid1002.030759

41. Sousa-Rocha D, Thomaz-Tobias M, Diniz LFA, Souza PSS, Pinge-Filho P, Toledo KA. Trypanosoma cruzi and its Soluble Antigens Induce NET Release by Stimulating Toll-Like Receptors. *PLoS One* (2015) **10**:e0139569. doi:10.1371/journal.pone.0139569

42. Porto BN, Alves LS, Fernández PL, Dutra TP, Figueiredo RT, Graça-Souza A V., Bozza MT. Heme Induces Neutrophil Migration and Reactive Oxygen Species Generation through Signaling Pathways Characteristic of Chemotactic Receptors. *J Biol Chem* (2007) **282**:24430–24436. doi:10.1074/jbc.M703570200

43. Mayadas TN, Cullere X, Lowell CA. The Multifaceted Functions of Neutrophils. *Annu Rev Pathol Mech Dis* (2014) **9**:181–218. doi:10.1146/annurev-pathol-020712-164023

44. Sabroe I, Prince LR, Jones EC, Horsburgh MJ, Foster SJ, Vogel SN, Dower SK, Whyte MKB. Selective Roles for Toll-Like Receptor (TLR)2 and TLR4 in the Regulation of Neutrophil Activation and Life Span. *J Immunol* (2003) **170**:5268–5275. doi:10.4049/jimmunol.170.10.5268

45. Kishimoto T, Jutila M, Berg E, Butcher E. Neutrophil Mac-1 and MEL-14 Adhesion Proteins Inversely Regulated by Chemotactic Factors. *Science (80-)* (1989) **245**:1238–1241. doi:10.1126/science.2551036

46. Zhou X, Gao XP, Fan J, Liu Q, Anwar KN, Frey RS, Malik AB. LPS activation, of Toll-like receptor 4 signals CD11b/CD18 expression in neutrophils. *Am J Physiol - Lung Cell Mol Physiol* (2005) **288**:L655-62. doi:10.1152/ajplung.00327.2004

47. Papayannopoulos V. Neutrophil extracellular traps in immunity and disease. *Nat Rev Immunol* (2018) **18**:134–147. doi:10.1038/nri.2017.105

48. Fischer MA, Davies ML, Reider IE, Heipertz EL, Epler MR, Sei JJ, Ingersoll MA, van Rooijen N, Randolph GJ, Norbury CC. CD11b+, Ly6G+ Cells Produce Type I Interferon and Exhibit Tissue Protective Properties Following Peripheral Virus Infection. *PLoS Pathog* (2011) **7**:e1002374. doi:10.1371/journal.ppat.1002374

49. Tate MD, Ioannidis LJ, Croker B, Brown LE, Brooks AG, Reading PC. The Role of Neutrophils during Mild and Severe Influenza Virus Infections of Mice. *PLoS One* (2011) **6**:e17618. doi:10.1371/journal.pone.0017618

50. Saitoh T, Komano J, Saitoh Y, Misawa T, Takahama M, Kozaki T, Uehata T, Iwasaki H, Omori H, Yamaoka S, et al. Neutrophil Extracellular Traps Mediate a Host Defense Response to Human Immunodeficiency Virus-1. *Cell Host Microbe* (2012) **12**:109–116. doi:10.1016/j.chom.2012.05.015

51. Muraro SP, De Souza GF, Gallo SW, Da Silva BK, De Oliveira SD, Vinolo MAR, Saraiva EM, Porto BN. Respiratory Syncytial Virus induces the classical ROS-dependent NETosis through PAD-4 and necroptosis pathways activation. *Sci Rep* (2018) **8**:14166. doi:10.1038/s41598-018-32576-y

52. Middleton EA, He XY, Denorme F, Campbell RA, Ng D, Salvatore SP, Mostyka M, Baxter-Stoltzfus A, Borczuk AC, Loda M, et al. Neutrophil Extracellular Traps (NETs) Contribute to Immunothrombosis in COVID-19 Acute Respiratory Distress Syndrome. *Blood* (2020) **136**:1169–1179. doi:10.1182/blood.2020007008

53. Heit B, Jones G, Knight D, Antony JM, Gill MJ, Brown C, Power C, Kubes P. HIV and Other Lentiviral Infections Cause Defects in Neutrophil Chemotaxis, Recruitment, and Cell Structure: Immunorestorative Effects of Granulocyte-Macrophage Colony-Stimulating Factor. *J Immunol* (2006) **177**:6405–6414. doi:10.4049/jimmunol.177.9.6405

54. Chen J, Yang YF, Yang Y, Zou P, Chen J, He Y, Shui SL, Cui YR, Bai R, Liang YJ, et al. AXL promotes Zika virus infection in astrocytes by antagonizing type I interferon signalling. *Nat Microbiol* (2018) **3**:302–309. doi:10.1038/s41564-017-0092-4

55. Giraldo DM, Hernandez JC, Velilla P, Urcuqui-Inchima S. HIV-1–neutrophil interactions trigger neutrophil activation and Toll-like receptor expression. *Immunol Res* (2016) **64**:93–103. doi:10.1007/s12026-015-8691-8

56. Hiroki CH, Toller-Kawahisa JE, Fumagalli MJ, Colon DF, Figueiredo LTM, Fonseca BALD, Franca RFO, Cunha FQ. Neutrophil Extracellular Traps Effectively Control Acute Chikungunya Virus Infection. *Front Immunol* (2020) **10**:3108. doi:10.3389/fimmu.2019.03108

57. Zanluqui N, Oliveira L, Polonio C, França T, De Souza G, Muraro S, Amorim M, Carregari V, Brandão-Teles C, da Silva P, et al. Zika Virus Infection of Murine and Human Neutrophils and their Function as Trojan Horses to the Placenta. *BioRxiv [Preprint]* (2021)

58. Bos S, Poirier-Beaudouin B, Seffer V, Manich M, Mardi C, Desprès P, Gadea G, Gougeon M-L. Zika Virus Inhibits IFN-α Response by Human Plasmacytoid Dendritic Cells and Induces NS1-Dependent Triggering of CD303 (BDCA-2) Signaling. *Front Immunol* (2020) **11**:582061. doi:10.3389/fimmu.2020.582061

59. Sun X, Hua S, Chen HR, Ouyang Z, Einkauf K, Tse S, Ard K, Ciaranello A, Yawetz S, Sax P, et al. Transcriptional Changes during Naturally Acquired Zika Virus Infection Render Dendritic Cells Highly Conducive to Viral Replication. *Cell Rep* (2017) **21**:3471–3482. doi:10.1016/j.celrep.2017.11.087

60. Aliota MT, Caine EA, Walker EC, Larkin KE, Camacho E, Osorio JE. Characterization of Lethal Zika Virus Infection in AG129 Mice. *PLoS Negl Trop Dis* (2016) **10**:e0004682. doi:10.1371/journal.pntd.0004682

61. Dowall SD, Graham VA, Rayner E, Atkinson B, Hall G, Watson RJ, Bosworth A, Bonney LC, Kitchen S, Hewson R. A Susceptible Mouse Model for Zika Virus Infection. *PLoS Negl Trop Dis* (2016) **10**:e0004658. doi:10.1371/journal.pntd.0004658

62. Lum FM, Narang V, Hue S, Chen J, McGovern N, Rajarethinam R, Tan JJL, Amrun SN, Chan

YH, Lee CYP, et al. Immunological observations and transcriptomic analysis of trimester-specific full-term placentas from three Zika virus-infected women. *Clin Transl Immunol* (2019) **8**:e1082. doi:10.1002/cti2.1082

63. Nguyen SM, Antony KM, Dudley DM, Kohn S, Simmons HA, Wolfe B, Salamat MS, Teixeira LBC, Wiepz GJ, Thoong TH, et al. Highly efficient maternal-fetal Zika virus transmission in pregnant rhesus macaques. *PLoS Pathog* (2017) **13**:e1006378. doi:10.1371/journal.ppat.1006378

64. Wang W, Li G, De W, Luo Z, Pan P, Tian M, Wang Y, Xiao F, Li A, Wu K, et al. Zika virus infection induces host inflammatory responses by facilitating NLRP3 inflammasome assembly and interleukin-1β secretion. *Nat Commun* (2018) **9**:106. doi:10.1038/s41467-017-02645-3

65. Frumence E, Roche M, Krejbich-Trotot P, El-Kalamouni C, Nativel B, Rondeau P, Missé D, Gadea G, Viranaicken W, Desprès P. The South Pacific epidemic strain of Zika virus replicates efficiently in human epithelial A549 cells leading to IFN-β production and apoptosis induction. *Virology* (2016) **493**:217–226. doi:10.1016/j.virol.2016.03.006

66. Hattar K, Franz K, Ludwig M, Sibelius U, Wilhelm J, Lohmeyer J, Savai R, Subtil FSB, Dahlem G, Eul B, et al. Interactions between neutrophils and non-small cell lung cancer cells: enhancement of tumor proliferation and inflammatory mediator synthesis. *Cancer Immunol Immunother* (2014) **63**:1297–1306. doi:10.1007/s00262-014-1606-z

67. Grandel U, Heygster D, Sibelius U, Fink L, Sigel S, Seeger W, Grimminger F, Hattar K. Amplification of Lipopolysaccharide-Induced Cytokine Synthesis in Non-Small Cell Lung Cancer/Neutrophil Cocultures. *Mol Cancer Res* (2009) **7**:1729–1735. doi:10.1158/1541-7786.MCR-09-0048

68. Serrao KL, Fortenberry JD, Owens ML, Harris FL, Brown LAS. Neutrophils induce apoptosis of lung epithelial cells via release of soluble Fas ligand. *Am J Physiol - Lung Cell Mol Physiol* (2001) **280**:L298-305. doi:10.1152/ajplung.2001.280.2.l298

69. Deng Y, Herbert JA, Robinson E, Ren L, Smyth RL, Smith CM. Neutrophil-Airway Epithelial Interactions Result in Increased Epithelial Damage and Viral Clearance during Respiratory Syncytial Virus Infection. *J Virol* (2020) **94**:e02161-19. doi:10.1128/jvi.02161-19

70. Pingen M, Bryden SR, Pondeville E, Schnettler E, Kohl A, Merits A, Fazakerley JK, Graham GJ, McKimmie CS. Host Inflammatory Response to Mosquito Bites Enhances the Severity of Arbovirus Infection. *Immunity* (2016) **44**:1455–1469. doi:10.1016/j.immuni.2016.06.002

71. Xu D, Wang P, Yang J, Qian Q, Li M, Wei L, Xu W. Gr-1+ Cells Other Than Ly6G+ Neutrophils Limit Virus Replication and Promote Myocardial Inflammation and Fibrosis Following Coxsackievirus B3 Infection of Mice. *Front Cell Infect Microbiol* (2018) **8**:157. doi:10.3389/fcimb.2018.00157

72. Kirsebom F, Michalaki C, Agueda-Oyarzabal M, Johansson C. Neutrophils do not impact viral load or the peak of disease severity during RSV infection. *Sci Rep* (2020) **10**:1110. doi:10.1038/s41598-020-57969-w

73. Cortjens B, Lutter R, Boon L, Bem RA, Van Woensel JBM. Pneumovirus-Induced Lung

Disease in Mice Is Independent of Neutrophil-Driven Inflammation. *PLoS One* (2016) **11**:e0168779. doi:10.1371/journal.pone.0168779

74. Wojtasiak M, Pickett DL, Tate MD, Londrigan SL, Bedoui S, Brooks AG, Reading PC. Depletion of Gr-1+, but not Ly6G+, immune cells exacerbates virus replication and disease in an intranasal model of herpes simplex virus type 1 infection. *J Gen Virol* (2010) **91**:2158–2166. doi:10.1099/vir.0.021915-0

75. Seo SU, Kwon HJ, Ko HJ, Byun YH, Seong BL, Uematsu S, Akira S, Kweon MN. Type I Interferon Signaling Regulates Ly6Chi Monocytes and Neutrophils during Acute Viral Pneumonia in Mice. *PLoS Pathog* (2011) **7**:e1001304. doi:10.1371/journal.ppat.1001304

76. Furuya Y, Steiner D, Metzger DW. Does type I interferon limit protective neutrophil responses during pulmonary Francisella tularensis infection? *Front Immunol* (2014) **5**:355. doi:10.3389/fimmu.2014.00355

77. Grant A, Ponia SS, Tripathi S, Balasubramaniam V, Miorin L, Sourisseau M, Schwarz MC, Sánchez-Seco MP, Evans MJ, Best SM, et al. Zika Virus Targets Human STAT2 to Inhibit Type I Interferon Signaling. *Cell Host Microbe* (2016) **19**:882–890. doi:10.1016/j.chom.2016.05.009

Figure Captions

Figure 1. ZIKV do not replicate in human neutrophils. **(A)** Neutrophils morphological features after isolation shown by flow cytometry and microscopy (bright-field, bar = 25 µm, magnification = 100x.). **(B)** The cells were stimulated *in vitro* during 2 hours with ZIKV BR 2015/15261, ZIKV PE243, ZIKV MR766 (1 MOI), or mock (C6/36 cells conditioned media in equivalent volume of ZIKV strains). Then, neutrophils were washed to remove the stimuli (indicated by ▼), and evaluated right after that (2 hours), and at 6, 12 and 24 hours after stimulation. When indicated, neutrophils were treated with trypsin after the wash step at 2 hours of stimulation with ZIKV strains. **(C)** Immunostaining of neutrophils with 4G2 (E protein; green) at 24 hours after ZIKV PE243 (a-d) or mock (e-h) stimulation. Nuclei (blue) were stained with Vybrant DyeCycleViolet. Merge of these stainings and the bright-field colocalization are also shown. C6/36 cells (l-p) were used as an infection positive control (bar = 50 µm, magnification = 40x.) **(D)** Histograms showing 4G2 intensity of fluorescence in neutrophils and C6/36 cells at 24 hours after mock and ZIKV PE243 stimulation as measured through flow cytometry. Infected-unstained cells were used as a negative fluorescence control. **(E)** Histograms showing AXL receptor intensity of fluorescence in neutrophils and A549 cells. An isotype control antibody was used as a negative fluorescence control. One representative result of three independent experiments is shown. **(F)** RNA levels of ZIKV strains in neutrophils at 2, 6, 12 and 24 hours after stimulation. **(G)** ZIKV loads on neutrophil culture supernatant at the same time after stimulation with ZIKV strains. The dashed line named input represents the mean of the titers of the three ZIKV strains still detected on the supernatant after the stimuli removal after 2 hours of stimulation. **(H)** RNA levels of ZIKV PE243 detected in neutrophils treated or not with trypsin after 2 hours of stimulation. Bars indicate standard error of the mean (SEM). Three-four independent experiments are shown (n = 9-15). The asterisk (*) denotes statistical difference between 6 and 12 hours of the ZIKV PE243 stimulation (F).

Figure 2. ZIKV mildly regulates CD62L expression in human neutrophils, but does not stimulate cytokines, elastase, and reactive oxygen species production by these cells. **(A)** Contour plots depicting the frequency of neutrophils $CD16^{+}CD11b^{+}$ and $CD16^{+}CD62L^{+}$ and the fluorescence intensity of CD11b and CD62L molecules inside these populations at 6 hours after stimulation with mock, LPS (100 ng/mL) or ZIKV PE243 (1 MOI). This time point and strain were chosen as a representative of these results. Isotype control antibodies were used as a negative fluorescence control to set the gates. A representative result of chloromethyl-H_2DCFDA (CM- H_2DCFDA)

fluorescence in the total neutrophil population at 6 hours after stimulation with mock, PMA (16 nM) or ZIKV PE243 is also shown. **(B)** Frequency of neutrophils $CD16^{+}CD11b^{+}$ and the mean fluorescence intensity (MFI) of CD11b in that population at 2, 6 and 12 hours after stimulation with mock, LPS or ZIKV strains (1 MOI). The dashed line represents the measurements right after neutrophil obtention from blood (0 hours). **(C)** Same analysis as in (B) applied to the CD62L molecule. **(D)** IL-8 levels in neutrophil culture supernatant at 6 and 12 hours after stimulation. **(E)** Elastase levels in neutrophil culture supernatant at 6 hours after stimulation. **(F)** Frequency of neutrophils CM-H_2DCFDA^{+} at 2 and 6 hours after stimulation. Bars indicate SEM. Two-three independent experiments are shown (n = 6-12). The asterisk (*) denotes statistical difference between mock and LPS (B-E) or PMA (F), and the number sign (#) between mock and all the three ZIKV strains in that time point (B-C).

Figure 3. ZIKV do not induce NETs, and are not captured by the DNA trap. **(A)** Immunostaining of neutrophils DNA (Vybrant DyeCycleViolet, blue) and acetyl-histone H3 (green) after 5 hours of stimulation with mock (a-d), PMA (160 nM) (e-h) or ZIKV PE243 (1 MOI) (i-l). ZIKV PE243 was chosen as representative of the ZIKV strains' effects. Merge of these stainings and the bright-field colocalization are also shown (bar = 50 µm, magnification = 60x). One representative of three independent experiments is shown. **(B)** Free double stranded DNA (dsDNA) on neutrophil culture supernatant after 5 hours of stimulation with mock, PMA or ZIKV strains (1 MOI). **(C)** ZIKV strains loads on neutrophil culture supernatant after 1 hour in the presence or absence of NETs induced by PMA stimulation during 5 hours. Bars indicate SEM. Two-three independent experiments are shown (n = 6-9). The asterisk (*) denotes statistical difference between mock and PMA (B).

Figure 4. Human neutrophil does not impair ZIKV infectivity. Frequency of $4G2^{+}$ A549 cells at 36 hours after infection with ZIKV strains (1 MOI) previously incubated 6 hours in the absence (ZIKV) or presence (ZIKV + NØ) of neutrophils. ZIKV PE243 is shown as a representative of the ZIKV strains' effects on the flow cytometry plots. The mock condition was used as a negative fluorescence control. Bars indicate SEM. Three independent experiments are shown (n = 9). (▼) indicates the moment A549 cells were washed to remove the virus. NØ = neutrophils.

Figure 5. ZIKV infection in human primary cells does not induce high levels IL-8 to promote migration of human neutrophils. **(A)** IL-8 levels in mdDCs and PBMCs culture supernatant at 24 and 48 hours after stimulation with mock, LPS (100 ng/mL), or ZIKV strains (1 MOI). **(B)** Chemotactic index of neutrophils after 2 hours of stimulation with 1,000 or 50,000 pg of rhIL-8, or the supernatant

of A549 cells culture pre-infected with ZIKV PE243 for 48 hours. Bars indicate SEM. Two-three independent experiments are shown (n = 6-9). The asterisk (*) denotes statistical difference between mock and LPS, and the number sign (#) between mock and all the three ZIKV strains in the time point.

Figure 6. Human neutrophils reduce ZIKV infection in A549 cells by contact. Flow cytometry plots depicting the frequency of $4G2^+$ A549 cells at 18 hours post-infection with ZIKV PE243 (1 MOI). Cells were infected for 2 hours in the absence of neutrophils (ZIKV), presence of neutrophils (ZIKV + NØ), or presence of trypsin pre-treated neutrophils (ZIKV + NØ-trypsin). ZIKV PE243 is shown as a representative of the ZIKV strains' effects. Mock condition was used as a negative fluorescence control. **(B)** Frequency of $4G2^+$ A549 cells at 18 hours post-infection with ZIKV strains (1 MOI) in the absence or presence of neutrophils. **(C)** Frequency of viable A549 cells (annexin V^-7-AAD^-) after 18 hours of infection with ZIKV PE243 (1 MOI) in the absence or presence to neutrophils during the infection. **(D)** Frequency of neutrophils $CD16^+CD11b^+$ and the mean fluorescence intensity (MFI) of CD11b in that population after the 2 hours of interaction with A459 cells stimulated with mock or PE243. **(E)** Same analysis as in (D) applied to the CD62L molecule. **(F)** Frequency of $4G2^+$ A549 cells at 18 hours post-infection with ZIKV PE243 in presence of trypsin pre-treated neutrophils. **(G)** ZIKV PE243 loads on A549 cells culture supernatant at 18 hours post-infection in presence of trypsin pre-treated neutrophils. Bars indicate SEM. Three-four independent experiments are shown (n = 7-15). The asterisk (*) denotes statistical difference between the absence and presence of neutrophils (B, F-G) or neutrophils pre-treated with trypsin (F) in the conditions. (▼) indicates the moment A549 cells were washed to remove the stimuli. NØ = neutrophils.

Figure 7. Trypsin treatment affects the expression of CD62L in neutrophils. **(A)** Frequency of viable neutrophils (annexin V^-7AAD^-) after treatment with trypsin. **(B)** Contour plots depicting the frequency of neutrophils $CD16^+CD11b^+$ and $CD16^+CD62L^+$ and the fluorescence intensity of CD11b and CD62L molecules inside these populations right after isolation from blood (NØ) or in trypsin pre-treated neutrophils (NØ-trypsin). Isotype control antibodies were used as a negative fluorescence control to set the gates. **(C)** Frequency of neutrophils $CD16^+CD11b^+$ and the mean fluorescence intensity (MFI) of CD11b in that population after treatment with trypsin. **(D)** Same analysis as in (C) applied to the CD62L molecule. Bars indicate SEM. Two independent experiments are shown (n = 6-7). The asterisk (*) denotes statistical difference between neutrophils treated or not with trypsin (D). NØ = neutrophils.

Figure 8. Mice neutrophil depletion does not restrict ZIKV relocation to draining lymph nodes. **(A)** ZIKV loads detected in the pool of both ipsi- and contralateral popliteal (pLN), sciatic (sLN) or lumbar aortic (laLN) lymph nodes per C57BL/6 mice after 10 minutes, 1 and 3 hours of ZIKV PE243 ($5x10^5$ FFU) injection in the footpad. **(B)** Flow cytometry plots depicting the frequency of PMN leukocytes $CD11b^+Ly6C/G^+$ in the total blood of mice 18 hours post-treatment with PBS or anti-Ly6G antibody (400 µg). **(C)** Frequency of $CD11b^+Ly6C/G^+$ cells in the PMN population in mice treated with PBS, anti-Ly6G, or an isotype antibody for 18 hours. **(D)** After neutrophil depletion, mice received a footpad subcutaneously injection of PBS or LPS (1000 ng) and 3 hours later, ZIKV PE243 ($5x10^5$ FFU). One hour later, ipsi- and contralateral pLNs from each mouse were harvested and pooled to determine ZIKV loads. Bars indicate SEM. Three animals per group were used in each experiment. One of three independent experiments is shown. The asterisk (*) denotes statistical difference between PBS and anti-Ly6G groups.

Supplementary Figure 1. ZIKV does not affect human neutrophil viability. **(A)** Contour plots depicting the frequency of annexin V^+ and 7-AAD^+ in the neutrophils gated population at 6 hours of stimulation with mock, LPS (100 ng/mL), or ZIKV PE243 (1 MOI), as a representative of the results. Mock-unstained condition was used as a negative control of fluorescence to set the gates. **(B)** Frequency of annexin V^+ and annexin V^+7-AAD^+ neutrophils at 2, 6, 12 and 24 hours of stimulation with mock, LPS, or ZIKV strains (1 MOI). The dashed line represents annexin V^+ and annexinV^+/7-AAD^+ frequency right after neutrophil purification from blood (0 hours). Bars indicate SEM. Three independent experiments are shown (n = 11). The asterisk (*) denotes statistical difference between mock and LPS and the number sign (#) between mock and all the three ZIKV strains in that time point.

Supplementary Figure 2. Human neutrophils reduce ZIKV infection in A549 cells previously infected with ZIKV. Frequency of $4G2^+$ A549 cells at 40 hours post-infection with ZIKV strains (1 MOI) when neutrophils were added or not to the previously infected A459 cells at 24 hours post-infection and left in contact with the culture for additional 16 hours. Bars indicate SEM. Three-four independent experiments are shown (n = 7-15). The asterisk (*) denotes statistical difference between the conditions in which neutrophils were present or absent. NØ = neutrophils.

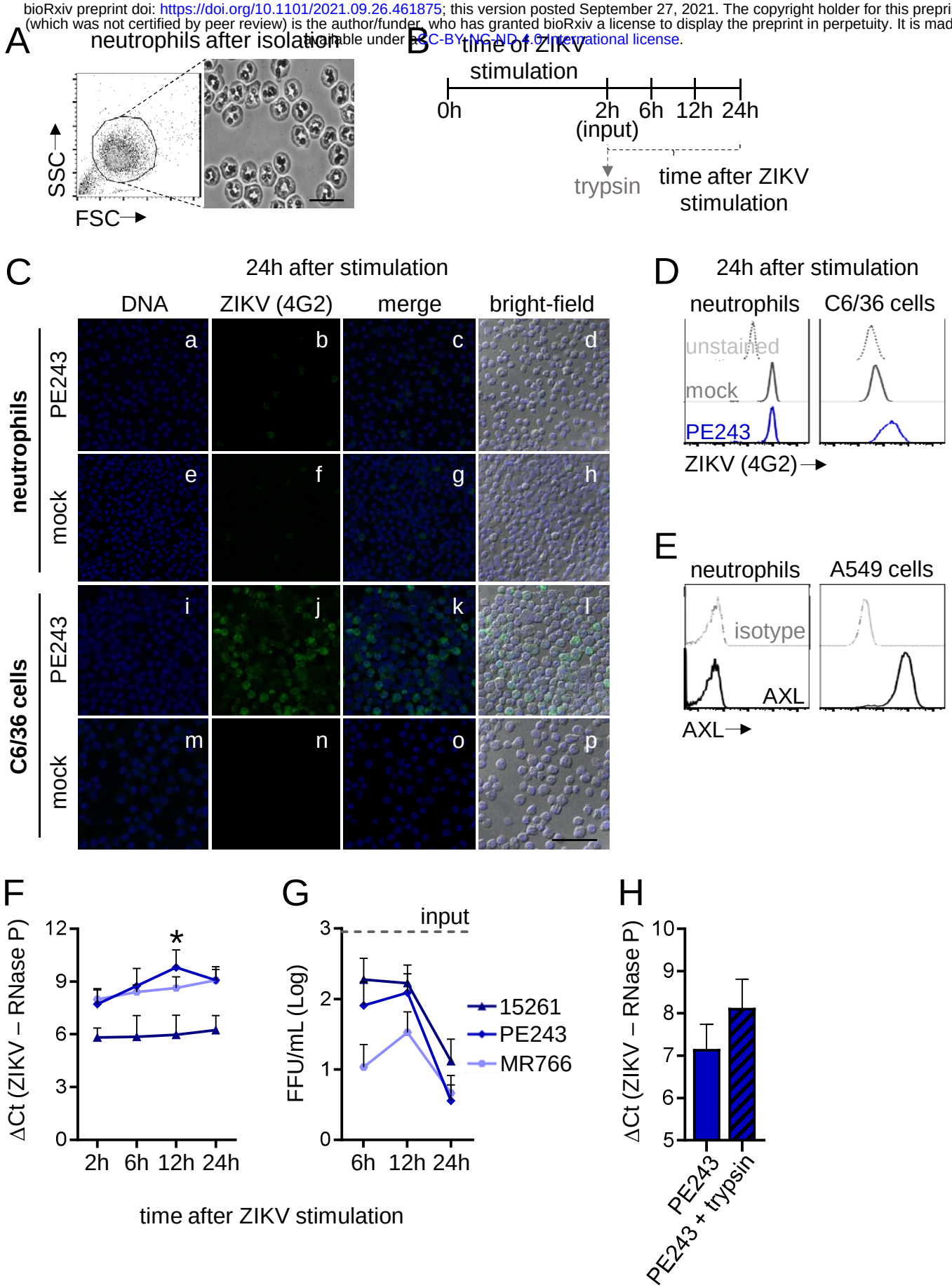

FIGURE 1

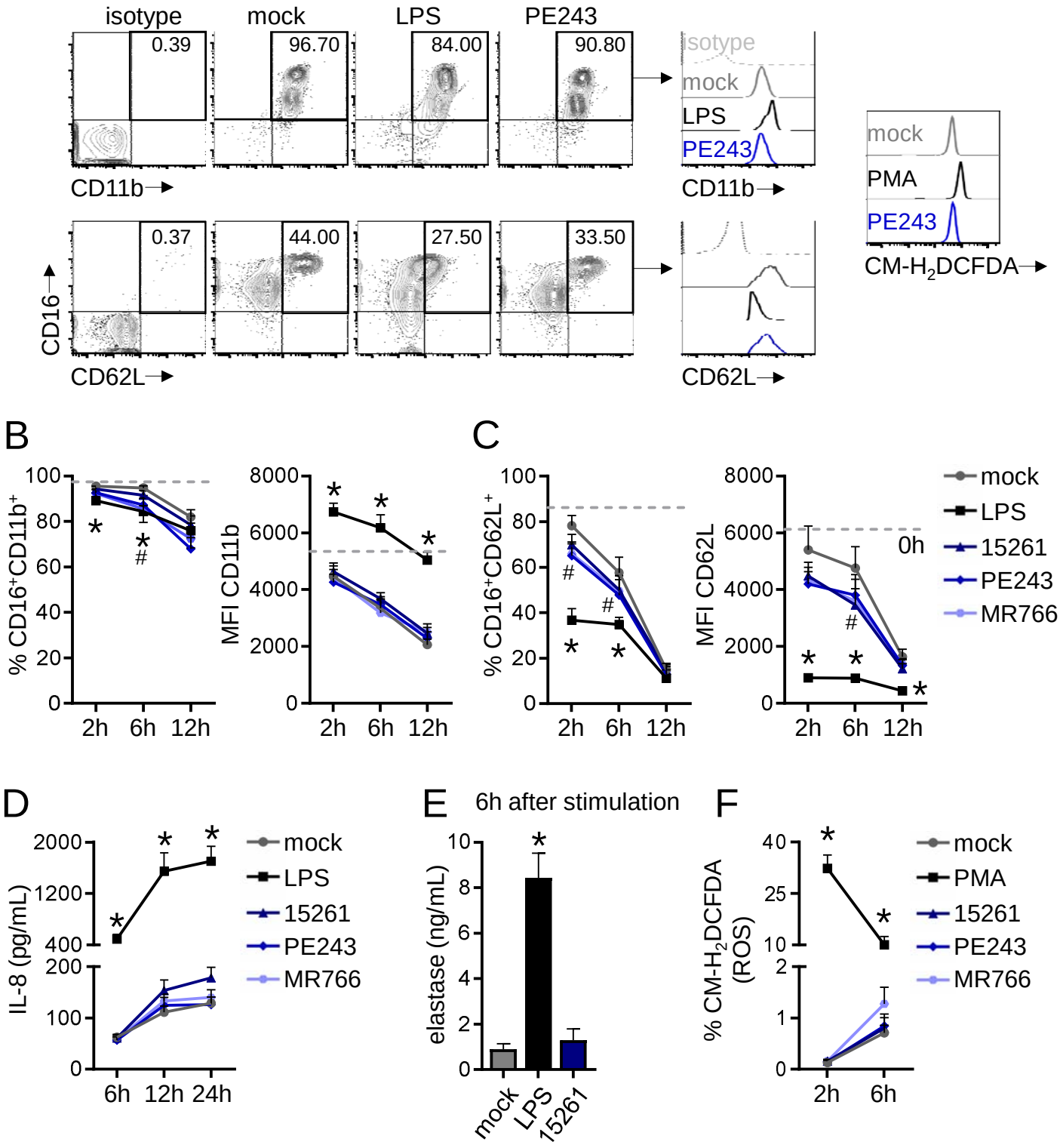

FIGURE 2

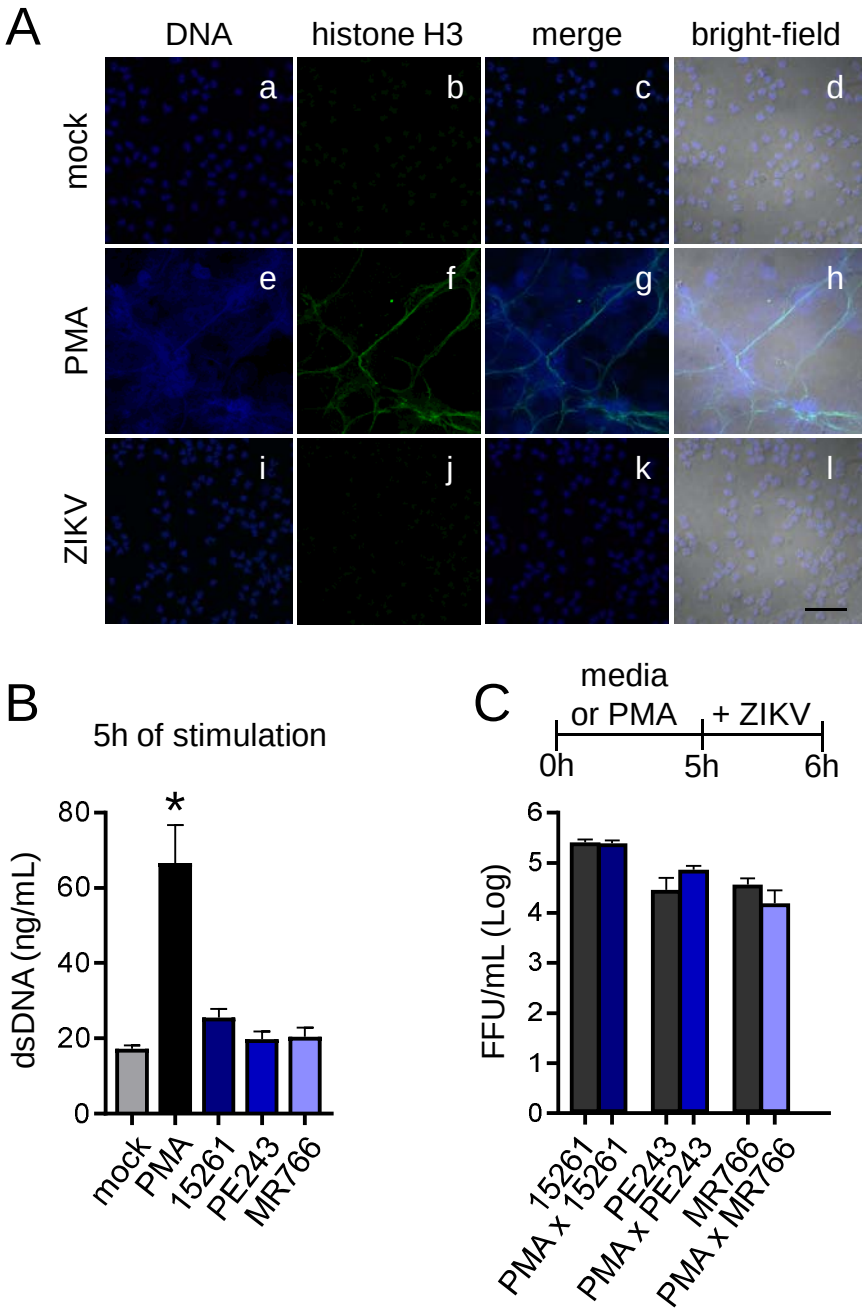

FIGURE 3

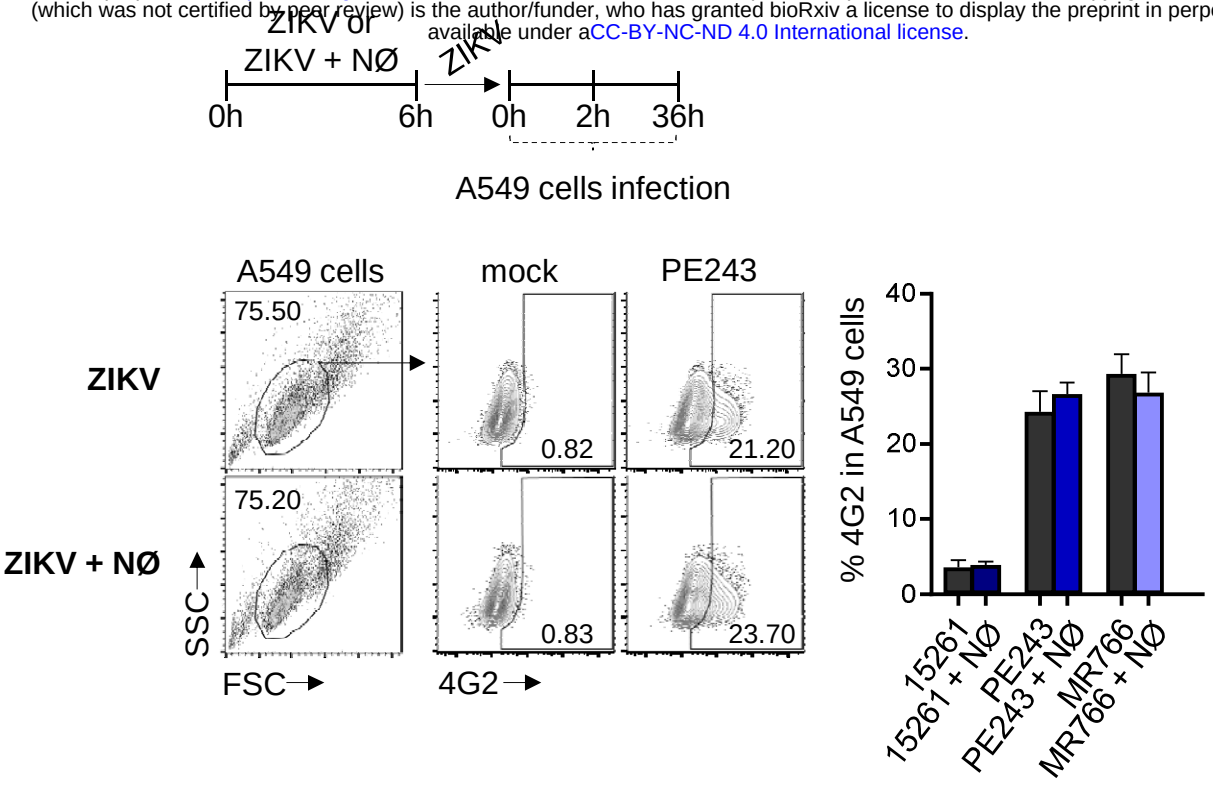

FIGURE 4

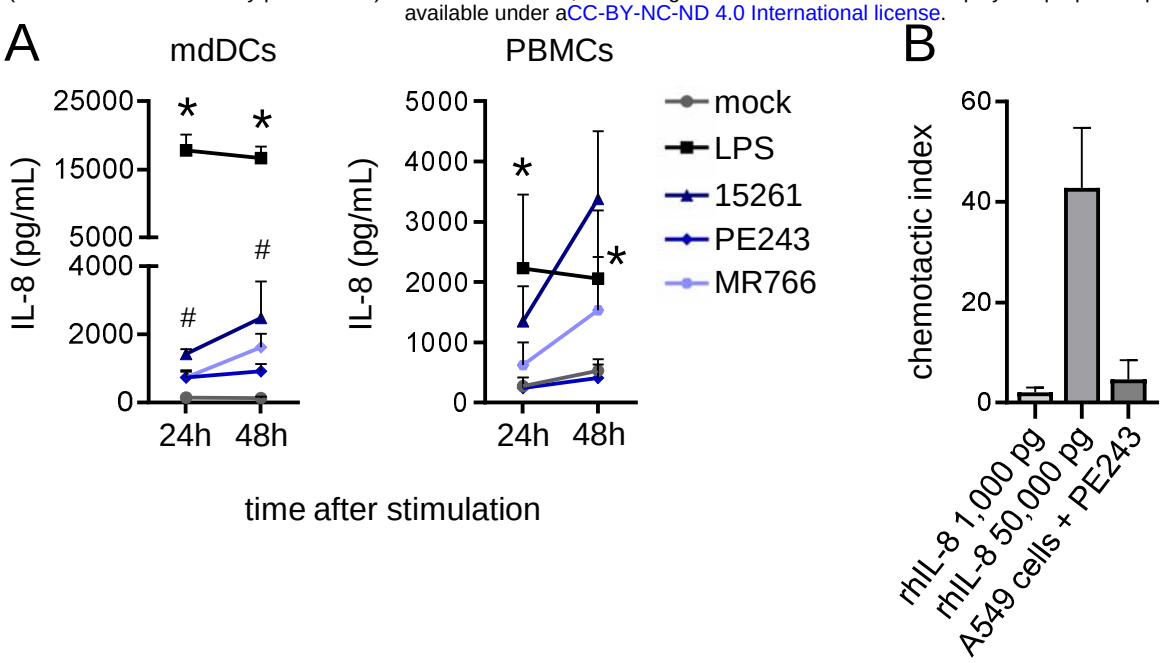

FIGURE 5

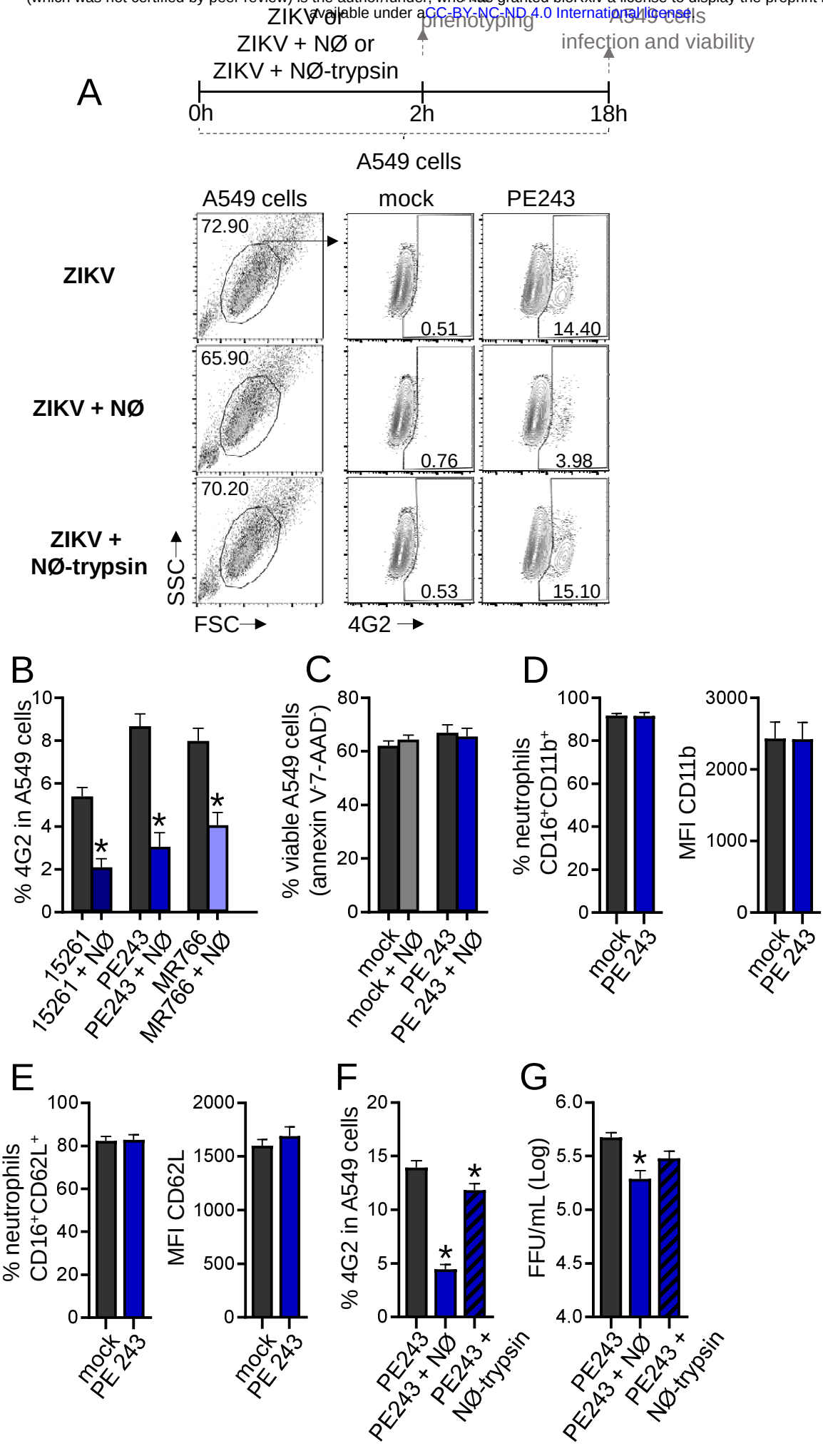

FIGURE 6

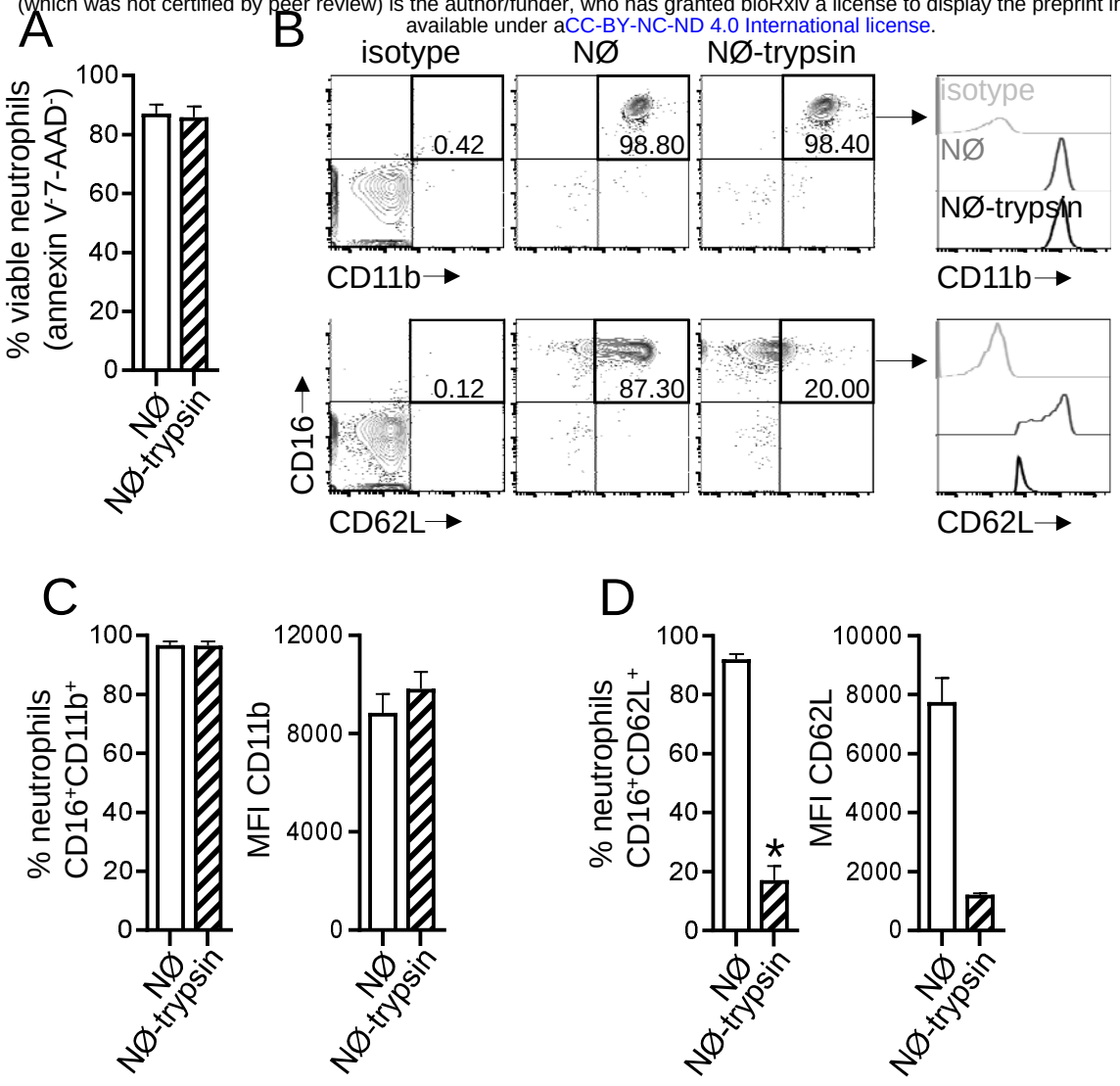

FIGURE 7

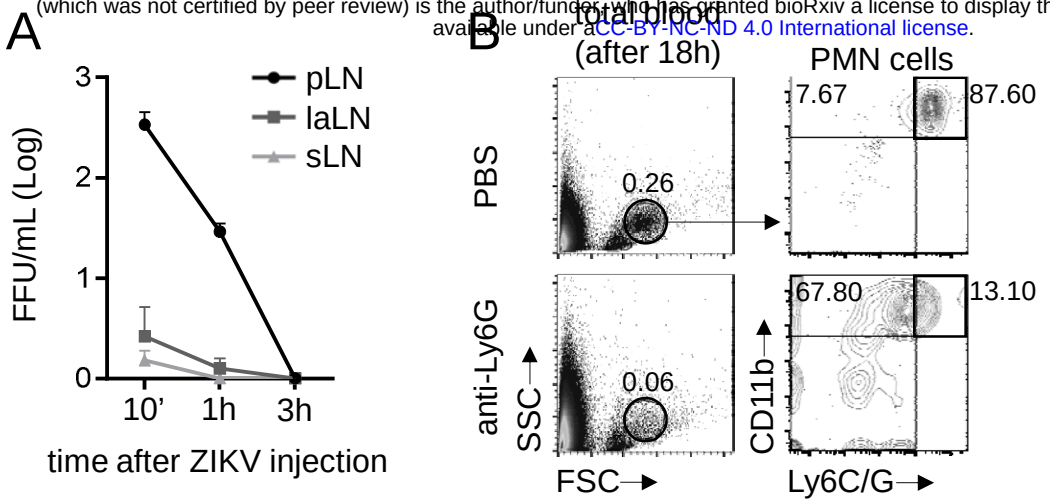

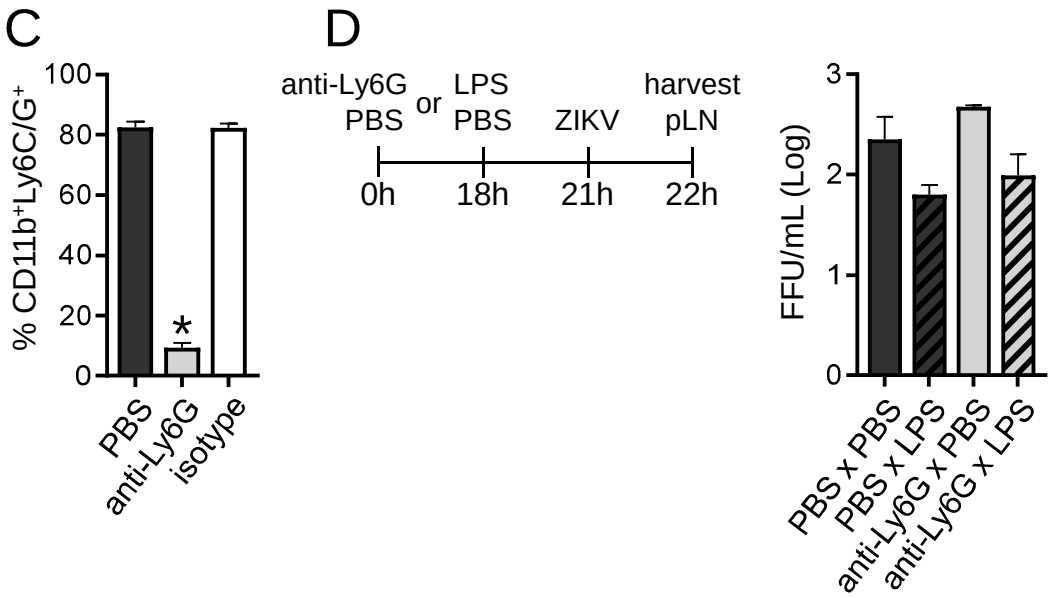

FIGURE 8

A

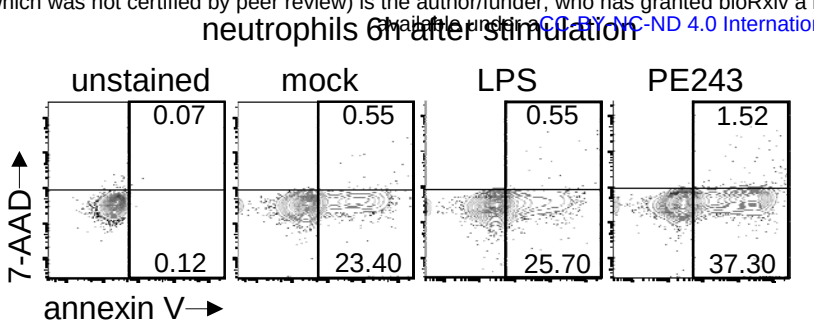

B

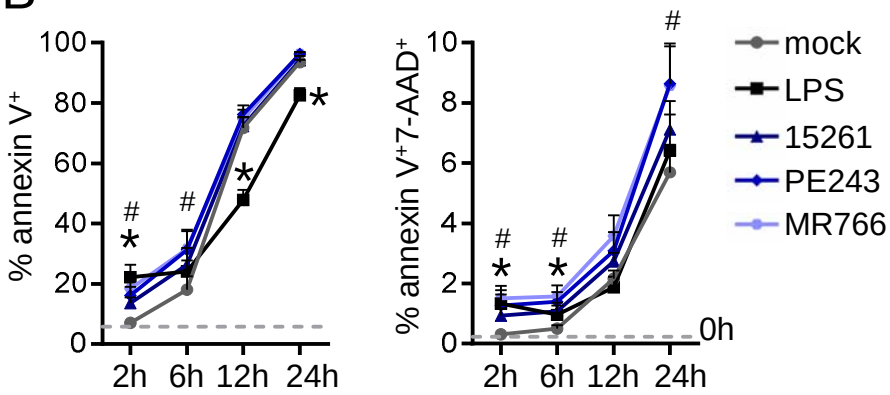

SUPPLEMENTARY FIGURE 1

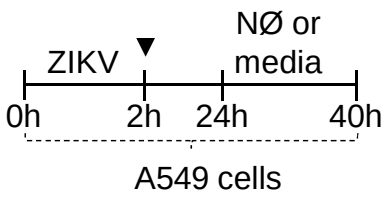

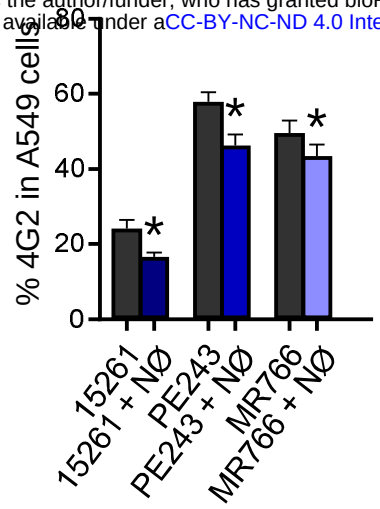

SUPPLEMENTARY FIGURE 2